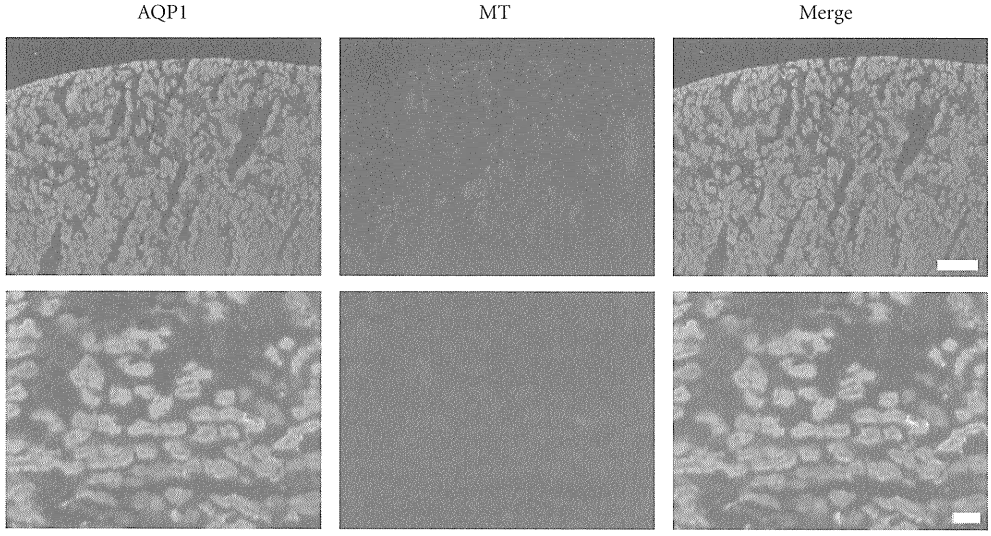

(a)

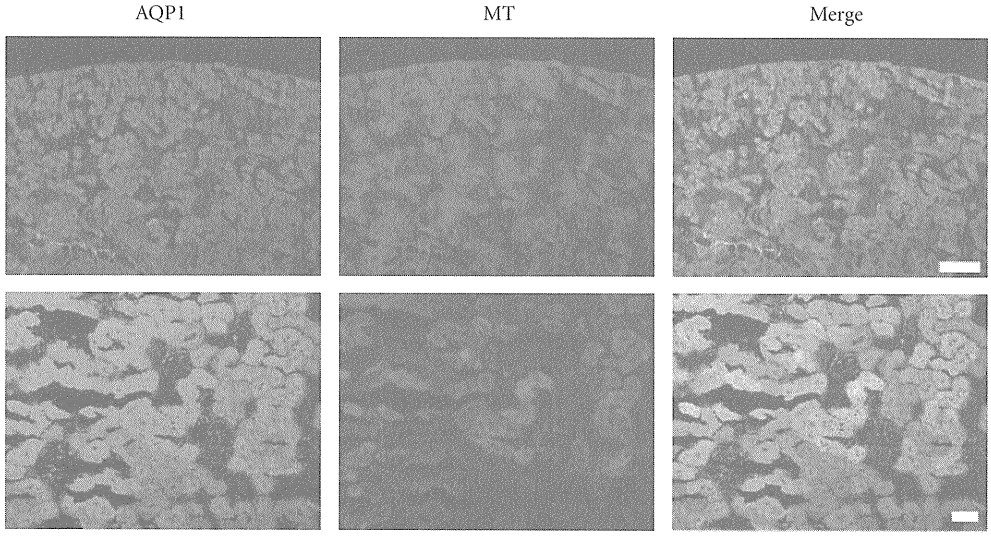

(b)

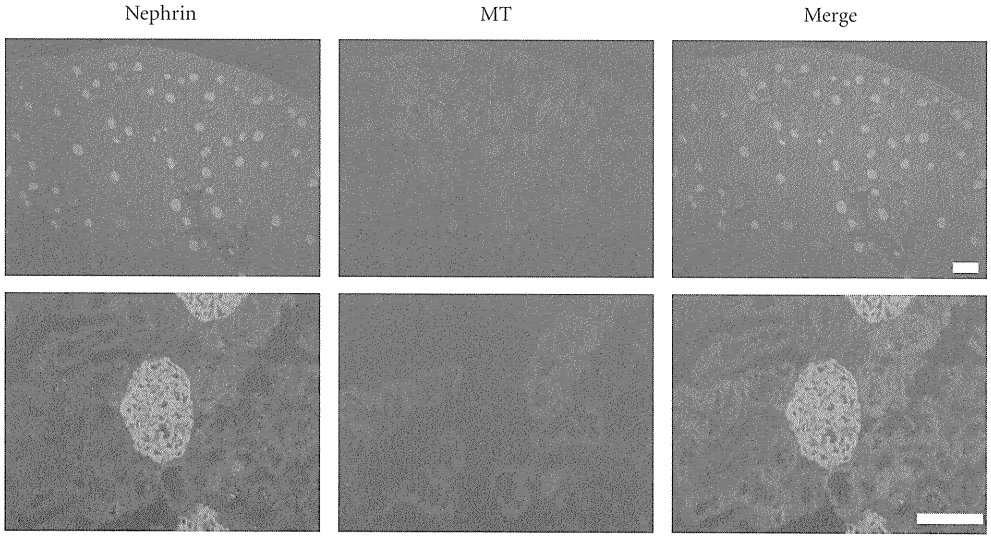

(c)

Figure 2: Continued.

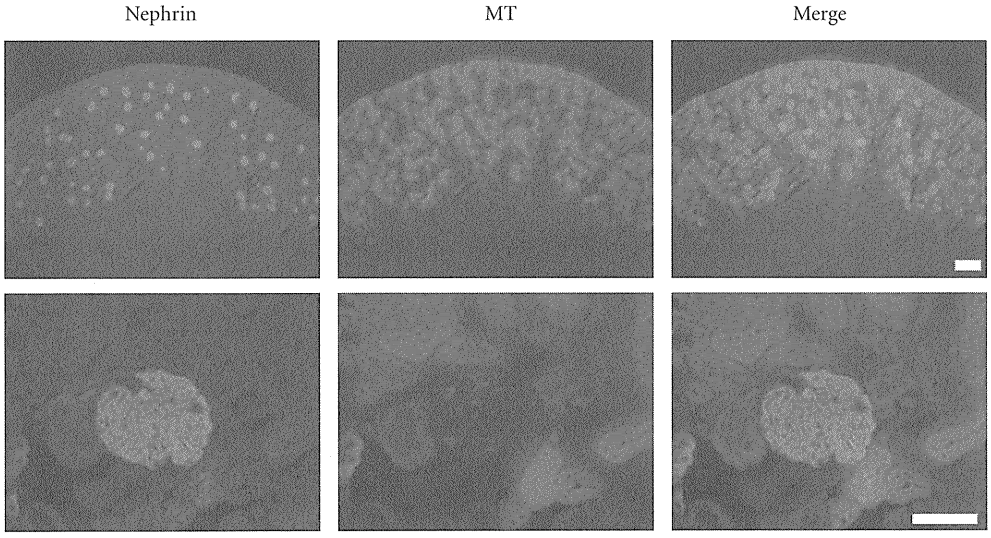

(d)

FIGURE 2: MT-1/-2 expression in podocytes and proximal tubular cells of the kidney. Immunofluorescent staining was performed as described in *Materials and Methods*. Eight weeks after inducing diabetes, MT-1/-2 was predominantly expressed in the proximal tubular epithelial cells of the kidney (b) and weakly expressed in podocytes (d) in the kidney of diabetic rats. In control rats, MT-1/-2 was weakly expressed in proximal tubular epithelial cells (a), but hardly in the podocytes (c). AQP1: aquaporin 1, MT: MT-1/-2. Scale bar: upper panels, 200 μm; lower panels, 50 μm.

C57BL/6J adult mouse kidney [20], were cultured in Dulbecco's modified Eagle's medium (Sigma-Aldrich Corp.) supplemented with 1000 mg/L D-glucose, 10% fetal bovine serum, 100 U/mL penicillin, and 100 mg/mL streptomycin at 37°C in 5% CO_2. To evaluate the effect of high glucose on MT expression, the cells were serum-starved by culture in 0.5% FBS for 24 h, then stimulated with 4500 mg/L D-glucose (high glucose) or D-mannitol (Sigma-Aldrich Corp.) for 24 h. For antioxidant treatment, the cells were pretreated with vitamin E (Sigma-Aldrich Corp.) at concentration ranges from 20 to 200 nM for 24 h, then stimulated with high glucose for 24 h. Individual experiments were repeated at least three times with different lots or preparations of cells.

2.4. Quantitative Analyses of MT-1 Gene and MT-1/-2 Protein Expression in mProx Cells. RNA was isolated from mProx cells using an RNeasy Mini kit (Qiagen, Valencia, CA). Single-strand cDNA was synthesized from the extracted RNA using a RT-PCR kit (Perkin Elmer, Foster City, CA). To evaluate the mRNA expression of MT-1 in mProx24 cells, quantitative RT-PCR (qRT-PCR) was performed using StepOnePlus (Applied Biosystems, Tokyo, Japan) and Fast-Start SYBR Premix Ex Taq II (Takara Bio Inc., Otsu, Japan). The primers for the MT-1 gene (upstream 5′-TCTAAGCGTCACCACGACTTCA-3′ and downstream 5′-GTGCACTTGCAGTTCTTGCAG-3′) were purchased from Takara Bio Inc. Each sample was analyzed in triplicate and normalized for GAPDH mRNA expression. Immunofluorescent staining of MT-1/-2 protein was performed as described above. The immunofluorescence intensity in cultured mProx cells was calculated using the formula, x (density) × positive area (μm^2), using Lumina Vision software (Mitani Corporation).

2.5. Statistical Analysis. All values are means ± SEM. Statistically significant differences between groups were examined using one-way ANOVA followed by Scheffé's test. Values of $P < 0.05$ were considered statistically significant.

3. Results

3.1. MT-1/-2 Expression Was Increased in Diabetic Kidney. MT-1/-2 expression was observed in the renal cortex from 1 week after the induction of diabetes. Its expression increased gradually and was strongly upregulated at week 8 (Figure 1,(d),(e),(f)). In contrast, MT-1/-2 was hardly detected in the kidney of control rats (Figure 1, (a),(b),(c)). Renal sections counterstained with antiaquaporin 1 and antinephrin antibodies revealed that MT-1/-2 expression was predominantly localized in the proximal tubular epithelial cells (Figure 2(b)), and to a lesser extent in the podocytes of the diabetic kidneys (Figure 2(d)). In control rats, MT-1/-2 was weakly expressed in the proximal tubular epithelial cells (Figure 2(a)), but not in the podocytes (Figure 2(c)). Body weight, kidney weight, UAE, and HbA1c are shown in Table 1. Diabetic rats had a significantly lower body weight and higher kidney weight per body weight at 8 weeks, but not at 1 and 2 weeks after the induction of diabetes. Similarly, The UAE and HbA1c level in the diabetic rats was significantly higher than in the control rats at 8 weeks, but not at 1 and 2 weeks. Glomerular hypertrophy and mesangial matrix expansion, but not interstitial changes and tubular atrophy

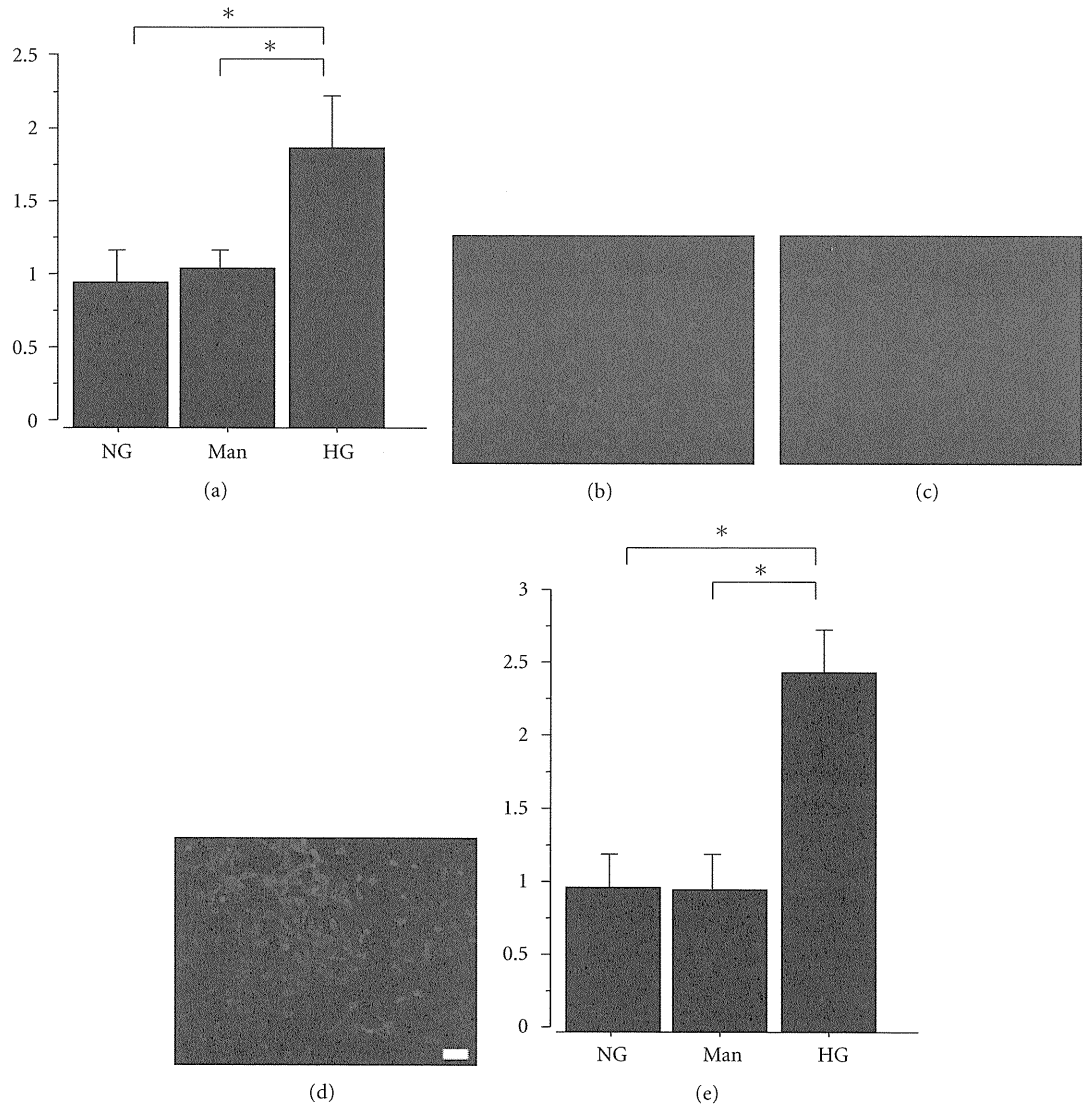

FIGURE 3: High glucose increases MT-1 mRNA and MT-1/-2 protein expression. mProx24 cells were serum-starved for 24 h before stimulation with high glucose or mannitol. (a) Cells were harvested after 24 h, and MT-1 mRNA expression was analyzed by qRT-PCR in three independent experiments and normalized for GAPDH. (b–e) MT-1/-2 protein expression was determined by immunofluorescent staining with anti-MT-1/-2 antibody 24 h after stimulation followed by densitometric analysis. Results are means ± SEM of three independent experiments. $^*P < 0.05$ versus high glucose; NG: normal glucose; Man: mannitol; HG: high glucose. Scale bar: 100 μm.

were observed in the diabetic rats as compared with control rats at 8 weeks (data not shown).

3.2. High Glucose Increased MT-1/-2 Expression in mProx24 Cells. qRT-PCR analyses revealed that exposure to the high glucose medium significantly increased MT-1 mRNA expression in mProx24 cells compared with normal glucose medium (Figure 3(a)). Similarly, high glucose, but not mannitol, significantly increased MT-1/-2 protein expression in mProx24 cells (Figures 3(b)–3(e)). These data indicate that high glucose increases the mRNA and protein expression of MT-1/-2 in mProx24 cells.

3.3. MT-1/-2 Expression Was Suppressed by Vitamin E. It is well known that high glucose increases the generation of ROS in various cells. To investigate the mechanism by which MT is induced by ROS in the high glucose condition, we examined the effects of an antioxidant, vitamin E, on MT-1/-2 expression in mProx24 cells. As shown in Figure 4, high-glucose-stimulated MT-1/-2 expression was significantly attenuated by vitamin E in a dose-dependent manner (Figure 4). Accordingly, these findings suggest that ROS generated by high glucose induces MT-1/-2 expression in the proximal tubular epithelial cells of the kidney.

4. Discussion

There is increasing evidence from experimental and clinical studies to suggest that oxidative stress plays a critical role in the pathogenesis and progression of diabetic

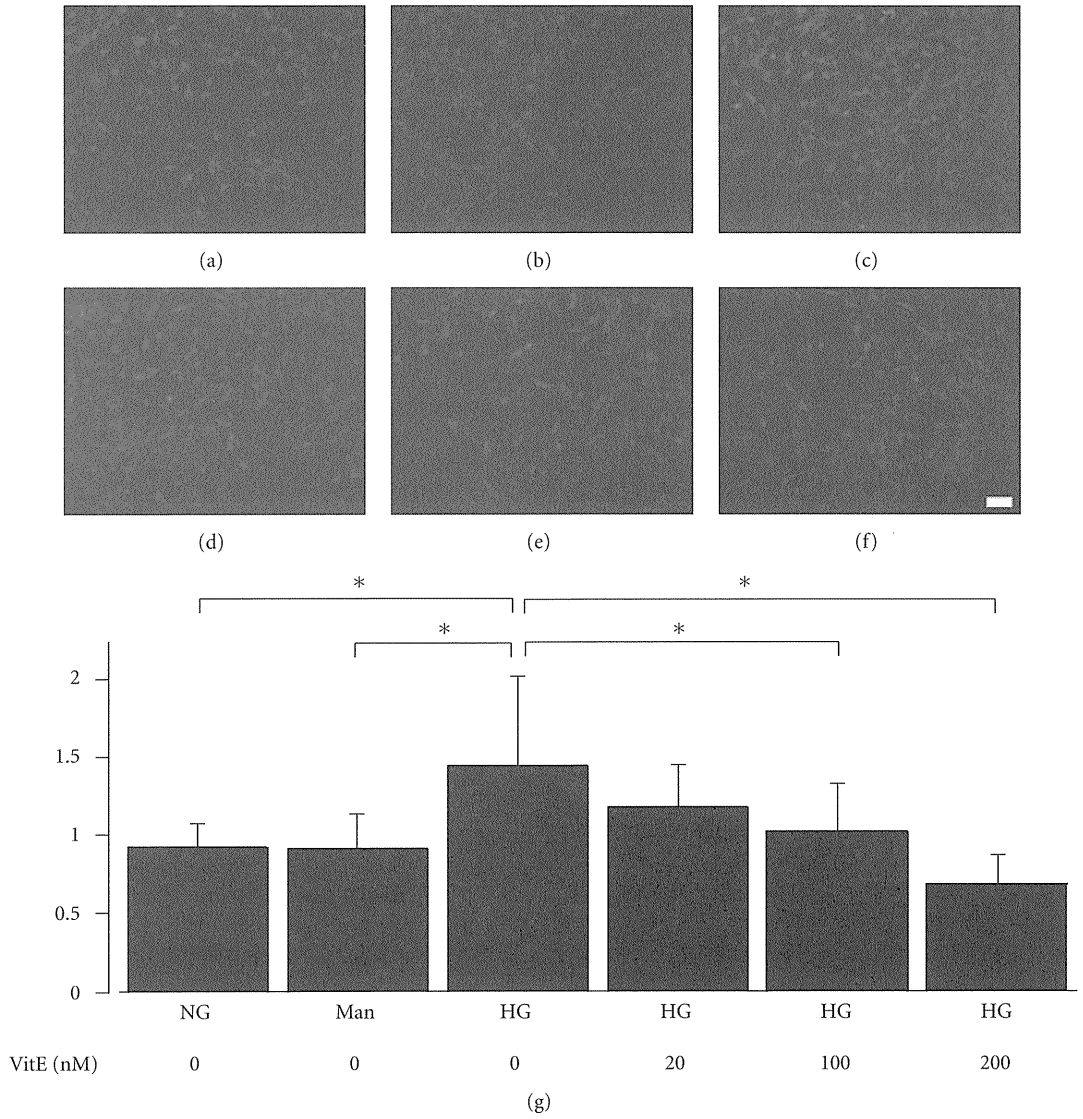

FIGURE 4: Vitamin E suppresses high glucose-induced MT-1/-2 expression. mProx24 cells were serum-starved and pretreated with vehicle or vitamin E for 24 h before stimulation with high glucose or mannitol. MT-1/-2 expression was determined by immunofluorescent staining. MT-1/-2 expression was not increased by mannitol (b) compared with normal glucose (a), but was increased by high glucose (c). High glucose-induced MT-1/-2 expression was attenuated by vitamin E pretreatment in a dose-dependent manner (d: 20 nM; E: 100 nM; F: 200 nM). The cells depicted are representative of three independent experiments. (g) Densitometric quantification of MT-1/-2 immunofluorescence. Results are means ± SEM of three independent experiments. $^*P < 0.05$ versus high glucose; NG: normal glucose; Man: mannitol; HG: high glucose; Vit E: vitamin E. Scale bar: 100 μm.

complications [21]. Since MT is a potent, endogenous and inducible antioxidant in various tissues [11, 12], we hypothesized that MT may be induced and act as an antioxidant in STZ-induced diabetic kidneys. Here, we found that high glucose induces the expression of MT-1/-2 mainly in proximal tubular epithelial cells and, to a lesser extent, in podocytes in rat kidneys. MT-1/-2 was dramatically expressed in renal proximal tubular epithelial cells within 1 week after inducing diabetes and gradually increased to week 8. MT-1/-2 expression seems to correlate with glucose level, but not with UAE, HbA1c, interstitial abnormalities. To our knowledge, this is the first report describing the localization and expression of MT-1/-2 in the diabetic kidney.

To elucidate the mechanism by which diabetes induces MT-1/-2 expression in proximal tubular epithelial cells, we investigated the effects of high glucose stimulation on mProx24, a murine renal proximal tubular epithelial cell line. We detected increased MT-1 mRNA and MT-1/-2 protein expression in the high glucose condition and found that high glucose-induced MT-1/-2 expression was suppressed by pretreatment with the antioxidant vitamin E. Vitamin E is well known to have high biological activity to protect cells from the propagation of free radical reactions [22, 23], thus we chose vitamin E in this study. These data suggest that ROS and oxidative stress, which are induced by high glucose, may be involved in the induction of MT-1/-2. Although

Table 1: Metabolic data at 1, 2, and 8 weeks after inducing diabetes.

	1 week	2 week	8 week
Body weight (g)			
Control	204 ± 6.3	241 ± 10.4	380 ± 13.3
Diabetic	198 ± 4.7	225 ± 11.5	248 ± 16.6*
Kidney weight (mg/g BW)			
Control	5.8 ± 0.4	5.6 ± 0.8	4.5 ± 0.7
Diabetic	5.9 ± 0.6	6.1 ± 1.0	6.7 ± 0.9*
UAE (μg/day)			
Control	110 ± 7.3	121 ± 8.1	137 ± 14.7
Diabetic	116 ± 5.7	125 ± 9.4	458 ± 24.5*
HbA1c (%)			
Control	3.7 ± 0.4	3.8 ± 0.6	3.8 ± 0.5
Diabetic	3.8 ± 0.3	4.3 ± 0.7	7.8 ± 0.9*

Data are means ± SEM; *$P < 0.05$ versus the control group. BW: body weight; UAE: urinary albumin excretion; HbA1c: hemoglobin A1c.

several studies have shown that MT protein expression is increased in the kidney of diabetic animals [16–18], the cellular distribution of MTs has not been addressed. Our data provide the first evidence for the expression profile of MT-1/-2 in the diabetic kidney. We speculate that MT-1/-2 is highly induced in proximal tubular epithelial cells in compensation for oxidative stress induced by high glucose.

Our study has potential limitations. First, we speculated that MT-1/-2 expression was upregulated by ROS, but further studies are needed to elucidate the underlying mechanisms. Although Zn is known to induce the gene and protein expression of MTs [24], this essential trace element is unlikely to be involved in our findings because the same chow was provided to the control and diabetic rats. In this study, we showed that high-glucose-stimulated MT-1/-2 expression was attenuated by vitamin E *in vitro*, but we have no data about diabetic rats treated by vitamin E. MT-1/-2 expression in the diabetic state may differ between cells and tissues, and the mechanisms by which other antioxidants regulate the expression of MT remain unclear. Further studies are needed to elucidate these issues. Second, it is still controversial whether site-specific induction of MT plays an important role in diabetic nephropathy. Podocyte-specific overexpression of MT reduced diabetic nephropathy in transgenic mice [25]. However, no studies have investigated whether MT expression in proximal tubular epithelial cells has a protective effect in diabetic animal models. Therefore, diabetes models using MT-knockout mice are needed to answer this question.

In conclusion, renal ROS, which are induced by diabetes, upregulate MT-1/-2 expression in proximal tubular epithelial cells of the kidney. Our results suggest that MT-1/-2 might be a novel therapeutic target to treat diabetic nephropathy.

Acknowledgments

This study was supported in part by a Grant-in-Aid for Young Scientists (B) from the Ministry of Education, Culture, Sports, Science and Technology, Japan, to Dr. Ogawa (21790813) and by a Grant-in-Aid for Diabetic Nephropathy from the Ministry of Health, Labour and Welfare of Japan. This work has received support from the Takeda Science Foundation and the Naito Foundation. The authors have no potential conflicts of interests relevant to this study to report.

References

[1] A. E. Declèves and K. Sharma, "New pharmacological treatments for improving renal outcomes in diabetes," *Nature Reviews Nephrology*, vol. 6, no. 6, pp. 371–380, 2010.

[2] J. W. Baynes and S. R. Thorpe, "Role of oxidative stress in diabetic complications: a new perspective on an old paradigm," *Diabetes*, vol. 48, no. 1, pp. 1–9, 1999.

[3] T. Nishikawa, D. Edelstein, X. L. Du et al., "Normalizing mitochondrial superoxide production blocks three pathways of hyperglycaemic damage," *Nature*, vol. 404, no. 6779, pp. 787–790, 2000.

[4] T. Matsuoka, J. Wada, I. Hashimoto et al., "Gene delivery of Tim44 reduces mitochondrial superoxide production and ameliorates neointimal proliferation of injured carotid artery in diabetic rats," *Diabetes*, vol. 54, no. 10, pp. 2882–2890, 2005.

[5] P. A. Craven, M. F. Melhem, S. L. Phillips, and F. R. DeRubertis, "Overexpression of Cu^{2+}/Zn^{2+} superoxide dismutase protects against early diabetic glomerular injury in transgenic mice," *Diabetes*, vol. 50, no. 9, pp. 2114–2125, 2001.

[6] F. R. DeRubertis, P. A. Craven, M. F. Melhem, and E. M. Salah, "Attenuation of renal injury in db/db mice overexpressing superoxide dismutase: evidence for reduced superoxide-nitric oxide interaction," *Diabetes*, vol. 53, no. 3, pp. 762–768, 2004.

[7] D. H. Hamer, "Metallothionein," *Annual Review of Biochemistry*, vol. 55, pp. 913–951, 1986.

[8] M. Vasak, "Advances in metallothionein structure and functions," *Journal of Trace Elements in Medicine and Biology*, vol. 19, no. 1, pp. 13–17, 2005.

[9] P. J. Thornalley and M. Vasak, "Possible role for metallothionein in protection against radiation-induced oxidative stress. Kinetics and mechanism of its reaction with superoxide and hydroxyl radicals," *Biochimica et Biophysica Acta*, vol. 827, no. 1, pp. 36–44, 1985.

[10] R. D. Palmiter, "The elusive function of metallothioneins," *Proceedings of the National Academy of Sciences of the United States of America*, vol. 95, no. 15, pp. 8428–8430, 1998.

[11] Y. J. Kang, Y. Chen, A. Yu, M. Voss-McCowan, and P. N. Epstein, "Overexpression of metallothionein in the heart of transgenic mice suppresses doxorubicin cardiotoxicity," *Journal of Clinical Investigation*, vol. 100, no. 6, pp. 1501–1506, 1997.

[12] A. R. Quesada, R. W. Byrnes, S. O. Krezoski, and D. H. Petering, "Direct reaction of H_2O_2 with sulfhydryl groups in HL-60 cells: zinc- metallothionein and other sites," *Archives of Biochemistry and Biophysics*, vol. 334, no. 2, pp. 241–250, 1996.

[13] M. Ebadi, H. Brown-Borg, H. El Refaey et al., "Metallothionein-mediated neuroprotection in genetically engineered mouse models of Parkinson's disease," *Molecular Brain Research*, vol. 134, no. 1, pp. 67–75, 2005.

[14] I. Miyazaki, M. Asanuma, H. Hozumi, K. Miyoshi, and N. Sogawa, "Protective effects of metallothionein against dopamine quinone-induced dopaminergic neurotoxicity," *FEBS Letters*, vol. 581, no. 25, pp. 5003–5008, 2007.

[15] I. Miyazaki, M. Asanuma, Y. Kikkawa et al., "Astrocyte-derived metallothionein protects dopaminergic neurons from

dopamine quinone toxicity," *Glia*, vol. 59, no. 3, pp. 435–451, 2011.

[16] M. L. Failla and R. A. Kiser, "Altered tissue content and cytosol distribution of trace metals in experimental diabetes," *Journal of Nutrition*, vol. 111, no. 11, pp. 1900–1909, 1981.

[17] M. L. Failla and C. Y. Gardell, "Influence of spontaneous diabetes on tissue status of zinc, copper, and manganese in BB Wistar rat," *Proceedings of the Society for Experimental Biology and Medicine*, vol. 180, no. 2, pp. 317–322, 1985.

[18] M. L. Kennedy and M. L. Failla, "Zinc metabolism in genetically obese (ob/ob) mice," *Journal of Nutrition*, vol. 117, no. 5, pp. 886–893, 1987.

[19] S. Okada, K. Shikata, M. Matsuda et al., "Intercellular adhesion molecule-1-deficient mice are resistant against renal injury after induction of diabetes," *Diabetes*, vol. 52, no. 10, pp. 2586–2593, 2003.

[20] S. Kitamura, Y. Maeshima, T. Sugaya, H. Sugiyama, Y. Yamasaki, and H. Makino, "Transforming growth factor-β 1 induces vascular endothelial growth factor expression in murine proximal tubular epithelial cells," *Nephron Experimental Nephrology*, vol. 95, no. 2, pp. e79–86, 2003.

[21] P. Rosen, P. P. Nawroth, G. King, W. Moller, H. J. Tritschler, and L. Packer, "The role of oxidative stress in the onset and progression of diabetes and its complications: a summary of a congress series sponsored by UNESCO-MCBN, the American diabetes association and the German diabetes society," *Diabetes/Metabolism Research and Reviews*, vol. 17, no. 3, pp. 189–212, 2001.

[22] E. Herrera and C. Barbas, "Vitamin E: action, metabolism and perspectives," *Journal of Physiology and Biochemistry*, vol. 57, no. 2, pp. 43–56, 2001.

[23] M. G. Traber and J. Atkinson, "Vitamin E, antioxidant and nothing more," *Free Radical Biology and Medicine*, vol. 43, no. 1, pp. 4–15, 2007.

[24] D. M. Alscher, N. Braun, D. Biegger et al., "Induction of metallothionein in proximal tubular cells by zinc and its potential as an endogenous antioxidant," *Kidney and Blood Pressure Research*, vol. 28, no. 3, pp. 127–133, 2005.

[25] S. Zheng, E. C. Carlson, L. Yang, P. M. Kralik, Y. Huang, and P. N. Epstein, "Podocyte-specific overexpression of the antioxidant metallothionein reduces diabetic nephropathy," *Journal of the American Society of Nephrology*, vol. 19, no. 11, pp. 2077–2085, 2008.

ORIGINAL ARTICLE

Activation of Peroxisome Proliferator–Activated Receptor δ Inhibits Streptozotocin-Induced Diabetic Nephropathy Through Anti-Inflammatory Mechanisms in Mice

Yuichi Matsushita,[1] Daisuke Ogawa,[1,2] Jun Wada,[1] Noriko Yamamoto,[1] Kenichi Shikata,[1,3] Chikage Sato,[1,2] Hiromi Tachibana,[1] Noriko Toyota,[1] and Hirofumi Makino[1]

OBJECTIVE—Activation of the nuclear hormone receptor peroxisome proliferator–activated receptor (PPAR)-δ has been shown to improve insulin resistance, adiposity, and plasma HDL levels. Several studies have reported that activation of PPARδ is atheroprotective; however, the role of PPARδ in renal function remains unclear. Here, we report the renoprotective effects of PPARδ activation in a model of streptozotocin-induced diabetic nephropathy.

RESEARCH DESIGN AND METHODS—Eight-week-old male C57BL/6 mice were divided into three groups: *1*) nondiabetic control mice, *2*) diabetic mice, and *3*) diabetic mice treated with the PPARδ agonist GW0742 (1 mg/kg/day). GW0742 was administered by gavage for 8 weeks after inducing diabetes.

RESULTS—GW0742 decreased urinary albumin excretion without altering blood glucose levels. Macrophage infiltration, mesangial matrix accumulation, and type IV collagen deposition were substantially attenuated by GW0742. The gene expression of inflammatory mediators in the kidney cortex, such as monocyte chemoattractant protein-1 (MCP-1) and osteopontin (OPN), was also suppressed. In vitro studies demonstrated that PPARδ activation increased the expression of anti-inflammatory corepressor B-cell lymphoma-6, which subsequently suppressed MCP-1 and OPN expression.

CONCLUSIONS—These findings uncover a previously unrecognized mechanism for the renoprotective effects of PPARδ agonists and support the concept that PPARδ agonists may offer a novel therapeutic approach for the treatment of diabetic nephropathy. ***Diabetes*** **60:960–968, 2011**

The increasing prevalence of diabetic nephropathy worldwide is a major societal issue because of the enormous expense associated with kidney replacement therapy (1). The pathogenesis of diabetic nephropathy is complex and involves multiple pathways that lead to kidney injury, including the polyol pathway (2), protein kinase C (3), advanced glycation end products (4), and transforming growth factor (TGF)-β (5). In addition, inflammation is now recognized to play an important role in the development of diabetic nephropathy (6,7). In this condition, the accumulation of macrophages and increased expression of cell adhesion molecules are observed in renal biopsy specimens from patients with diabetic nephropathy (8). We have demonstrated that inflammation in diabetic nephropathy can be ameliorated by inhibiting macrophage infiltration in intercellular adhesion molecule-1 (ICAM-1) and macrophage scavenger receptor-A (SR-A) knockout mice (9,10). Therefore, inflammation could be a major therapeutic target of diabetic nephropathy.

There is an increasing body of evidence suggesting that a subfamily of nuclear hormone receptor transcription factors, namely the peroxisome proliferator–activated receptors (PPARs) (PPARγ, PPARα, and PPARδ), may play important roles in the pathogenesis of metabolic syndrome, obesity, and diabetes (11). PPARs are also implicated in many renal pathophysiological conditions, including diabetic nephropathy and glomerulosclerosis (12). Synthetic PPARγ and PPARα agonists, such as thiazolidinediones and fibrates, improve the glycemic control in type 2 diabetic patients and lower the serum triglyceride levels in hyperlipidemic patients. In addition, we and other investigators have reported that PPARγ and PPARα agonists are also beneficial in diabetic nephropathy (13–15). Although atheroprotective effects of PPARδ agonists have been reported (16,17), there are no reports regarding the effects of PPARδ agonists on diabetic nephropathy.

The purpose of the current study was to investigate the hypothesis that activation of PPARδ prevents the development of diabetic nephropathy by inhibiting inflammatory processes, including chemokine/cytokine expression and macrophage infiltration.

RESEARCH DESIGN AND METHODS

Experimental protocol. Male C57BL/6J mice were purchased from Charles River (Yokohama, Japan). Eight-week-old mice were divided into three groups: *1*) nondiabetic control mice (control; $n = 6$), *2*) streptozotocin (STZ)–induced diabetic mice (DM; $n = 7$), and *3*) diabetic mice treated with PPARδ agonist GW0742 (DM+GW0742; $n = 7$). GW0742 mice were purchased from Sigma-Aldrich (Tokyo, Japan). Diabetes was induced by peritoneal injection of 200 mg/kg STZ (Sigma-Aldrich) in citrate buffer (pH 4.5). Blood glucose was measured by the glucose oxidase method at 3 and 7 days after STZ injection, and only mice with blood glucose concentrations >16 mmol/L were used in the study. Mice in the control group were injected with citrate buffer. The DM+GW0742 group received 1 mg/kg/day of GW0742 by gavage for 8 weeks. All mice had free access to standard diet and tap water. All procedures were performed according to the Guidelines for Animal Experiments at Okayama University Medical School, Japanese Government Animal Protection and Management Law (No. 105), and Japanese Government Notification on Feeding and Safekeeping of Animals (No. 6). Mice were killed at 8 weeks after

From the [1]Department of Medicine and Clinical Science, Okayama University Graduate School of Medicine, Dentistry and Pharmaceutical Sciences, Okayama, Japan; the [2]Department of Diabetic Nephropathy, Okayama University Graduate School of Medicine, Dentistry and Pharmaceutical Sciences, Okayama, Japan; and the [3]Center for Innovative Clinical Medicine, Okayama University Hospital, Okayama, Japan.
Corresponding author: Daisuke Ogawa, daiogawa@md.okayama-u.ac.jp.
Received 24 September 2010 and accepted 16 December 2010.
DOI: 10.2337/db10-1361

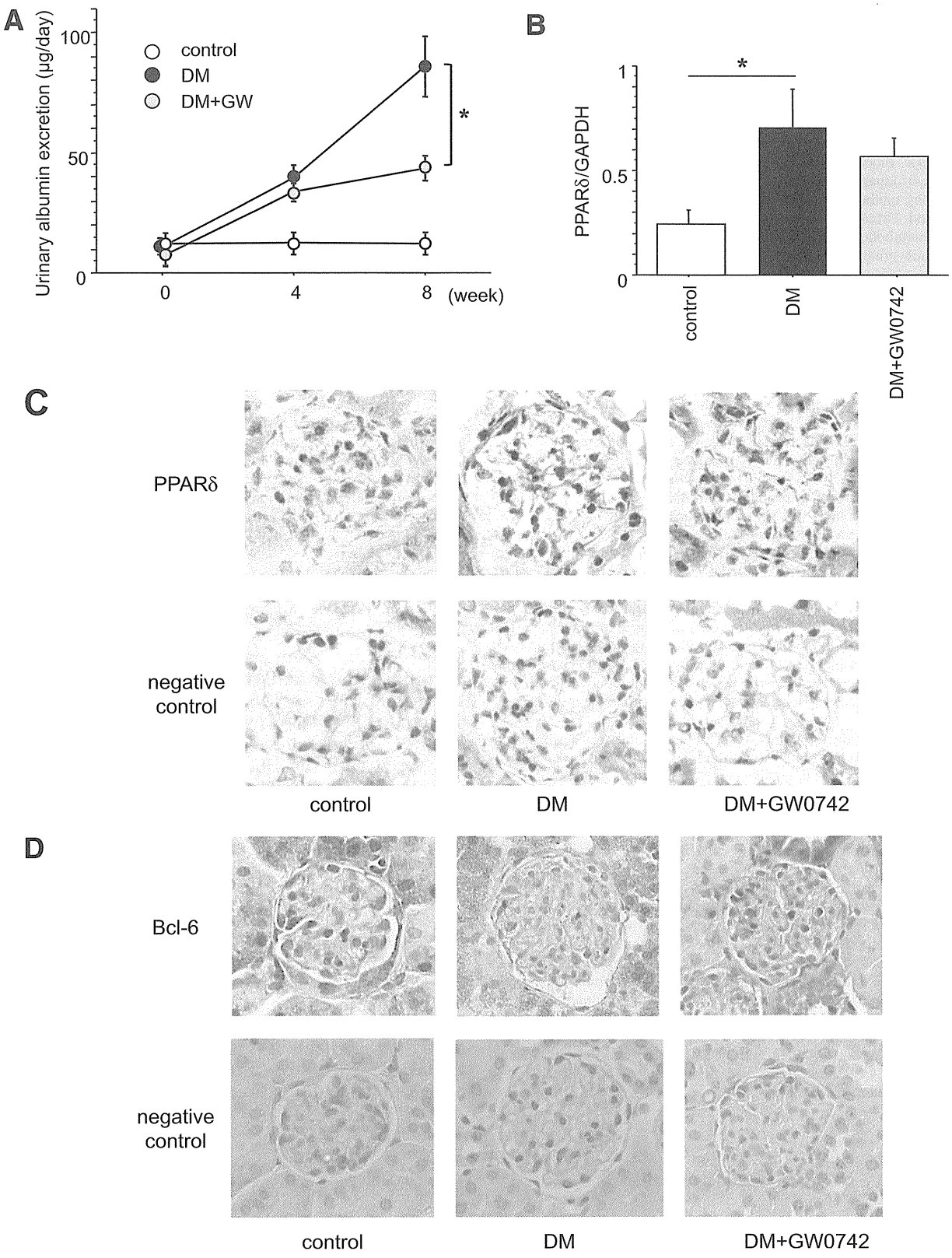

FIG. 1. Time course of changes in UAE and PPARδ mRNA and protein expression in the kidneys. *A*: The UAE increased progressively in the untreated diabetic (DM) group during the 8-week observation period after the induction of diabetes. GW0742 treatment (DM+GW0742) significantly reduced UAE at 8 weeks compared with the DM group. Control, nondiabetic control mice. Data are means ± SE. *$P < 0.01$ for DM vs. DM+GW0742. *B*: Renal PPARδ mRNA expression was significantly increased in the DM group compared with the control group. Data are means ± SE. *$P < 0.05$. *C*: Localization of renal PPARδ protein expression by immunohistochemistry. PPARδ protein expression was predominantly localized in the glomeruli of the DM and DM+GW0742 groups. Original magnification ×400. *D*: Localization of renal Bcl-6 protein expression by immunohistochemistry. Bcl-6 protein was mainly expressed in the glomeruli of the control group, but its expression was suppressed in the DM group. The expression of Bcl-6 recovered in the DM+GW0742 groups compared with the DM group. Original magnification ×400. (A high-quality digital representation of this figure is available in the online issue.)

inducing diabetes. The kidneys were removed, weighed, and fixed in 10% formalin for periodic acid–methenamine silver (PAM) staining, and parts of the remaining tissues were embedded in optimal cutting temperature compound (Sakura Finetechnical, Tokyo, Japan) and frozen immediately in acetone cooled on dry ice. Other tissues were snap-frozen in liquid nitrogen and stored at −80°C.

Metabolic data. We measured body weight, blood pressure, hemoglobin A_{1c} (HbA_{1c}), 24-h urinary albumin excretion (UAE), and creatinine clearance at 0, 4, and 8 weeks. Blood pressure was measured using the tail-cuff method (Softron, Tokyo, Japan). HbA_{1c} was measured using the high-pressure liquid chromatography method, and serum creatinine was measured using the enzymatic method. Urine was collected for 24 h, with each mouse individually housed in a metabolic cage and provided with food and water ad libitum. Urinary albumin concentration was measured as previously described (9). Creatinine was measured enzymatically, and creatinine clearance was calculated.

Light microscopy. PAM-stained sections were analyzed. To evaluate glomerular size, we examined 10 randomly selected glomeruli in the cortex per animal under high magnification (×400) at 8 weeks after induction of diabetes. The area of the glomerular tuft and the mesangial matrix index (MMI) were measured using Lumina Vision software (Mitani Corporation, Tokyo, Japan). MMI was defined as the PAM-positive area in the tuft area, calculated using the following formula: MMI = (PAM positive area)/(tuft area). The results are expressed as means ± SE (per μm^2 for tuft area; arbitrary units for MMI).

Immunoperoxidase staining. Immunoperoxidase staining was performed as previously described (9). Briefly, fresh frozen sections were cut to 4 μm thick using a cryostat. To evaluate macrophage infiltration, we applied a rat anti-mouse monocyte/macrophage (F4/80) monoclonal antibody (Abcam, Tokyo, Japan), followed by biotin-labeled goat antirat IgG antibody (Jackson Immunoresearch Laboratories, West Grove, PA). The avidin-biotin coupling reaction was performed on sections using a Vectastain Elite kit (Vector Laboratories, Burlingame, CA). We examined 10 glomeruli per animal and counted the number of F4/80-positive cells. The mean number of positive cells per glomerulus and interstitial tissue (number per mm^2) were used for the estimation. To evaluate PPARδ and Bcl-6 expression, PPARδ rabbit polyclonal antibody (Affinity BioReagents, Golden, CO) and Bcl-6 rabbit polyclonal antibody (Santa Cruz Biotechnology, Santa Cruz, CA) were applied, followed by biotin-labeled donkey anti-rabbit IgG antibody (Jackson Immunoresearch Laboratories).

Immunofluorescent staining. Immunofluorescent staining was performed as previously described (9). To clarify the differences in mesangial matrix proteins, we used rabbit anti-type IV collagen antibody (Millipore, Temecula, CA), followed by Alexa Fluor 488 goat anti-rabbit IgG (Invitrogen, Carlsbad, CA). Fluorescence pictures were obtained using a fluorescence microscope (BX51; Olympus, Tokyo, Japan). The type IV collagen immunofluorescence intensity was quantified as previously described (9). Briefly, using Lumina Vision software (Mitani Corporation), the intensity of expression on the images was calculated using the formula, x (density) × positive area (μm^2). The positive area of type IV collagen in each glomerulus was estimated as the ratio to the mean area of the glomerulus. Ten glomeruli per animal were evaluated.

Quantitative analysis of renal cortex gene expression. The RNA from the renal cortex was isolated 8 weeks after treatment using an RNeasy Mini Kit (Qiagen, Valencia, CA). Single-strand cDNA was synthesized from the extracted RNA using a RT-PCR kit (Perkin Elmer, Foster City, CA). To evaluate the mRNA expression of PPARδ, CD14, CD11c, monocyte chemoattractant protein (MCP)-1, chemokine CC motif receptor 2 (CCR2), TGF-β, tumor necrosis factor (TNF)-α, osteopontin (OPN), and ICAM-1 in the renal cortex, quantitative RT-PCR (qRT-PCR) was performed using StepOnePlus (Applied Biosystems, Tokyo, Japan) and FastStart SYBR Premix Ex Taq II (Takara Bio, Otsu, Japan). The primers were purchased from Takara Bio. Each sample was analyzed in triplicate and normalized for GAPDH mRNA expression.

Cell culture and treatment. RAW 264.7 murine macrophages were cultured in Dulbecco's modified Eagle's medium supplemented with 1,000 mg/L D-glucose, 10% FBS, 100 units/mL penicillin, 100 mg/mL streptomycin, and 2 mmol/L L-glutamine. For ligand treatment, cells were serum-starved by culture in 0.5% FBS for 24 h. After pretreatment with GW0742 (10 μmol/L) for 24 h, the cells were stimulated with 4,500 mg/L D-glucose (high glucose) for 24 h. Individual experiments were repeated at least three times with different lots or preparation of cells.

Quantitative analysis of gene expression in RAW macrophages. Total RNA was prepared from cells using an RNeasy Mini Kit (Qiagen) as described above. B-cell lymphoma-6 (Bcl-6), MCP-1, and OPN mRNA expression in RAW macrophages was measured using qRT-PCR, as described above.

Immunoprecipitation and Western blotting. Bcl-6 and PPARδ protein expression levels were determined by Western blotting. To examine the interactions between PPARδ and Bcl-6, the nuclear protein fraction was isolated from RAW macrophages using a Nuclear Extract Kit (Active Motif, Carlsbad, CA). The nuclear protein was immunoprecipitated with an anti-PPARδ antibody (Affinity BioReagents) for 1.5 h at 4°C. The nuclear protein–antibody complex was then incubated with magnetized Protein G Dynabeads (Invitrogen) for 45 min at room temperature. After washing the beads, the bound proteins were eluted and resolved by SDS-PAGE. Protein was transferred to nitrocellulose membranes and blocked in 20 mmol/L Tris-HCl (pH 7.6) containing 150 mmol/L NaCl, 0.1% Tween-20, and 5% (wt/vol) nonfat dried milk. The blots were then incubated with anti-PPARδ antibody (Affinity BioReagents) and anti–Bcl-6 antibody (Santa Cruz Biotechnology). The immunoblots were hybridized with anti-TATA binding protein antibody (Abcam) to monitor equivalent loading in different lanes. All experiments were repeated at least three times.

Statistical analysis. All values are means ± SE. Statistically significant differences between groups were examined using one-way ANOVA followed by Scheffé test. A P value <0.05 was considered statistically significant.

RESULTS

Metabolic data and time course of changes in UAE. The UAE progressively increased in diabetic mice during the study (Fig. 1*A*). However, GW0742 treatment significantly reduced the mean UAE (86.09 ± 12.67 μg/day) compared with the DM group at 8 weeks after inducing diabetes (40.91 ± 3.94 μg/day; $P < 0.01$). The other metabolic data are summarized in Table 1. Eight weeks after inducing diabetes, there were no significant differences in systolic blood pressure between the three groups. HbA_{1c}, kidney weight, and relative kidney weight were significantly higher in the DM group than in the control group. There was no significant difference in HbA_{1c}, kidney weight, and relative kidney weight between the DM and the DM+GW0742 groups. Body weight was lower in both the DM and the DM+GW0742 groups than in the control, but was higher in the DM+GW0742 than in the DM group. There were no significant differences in creatinine clearance or triglyceride levels between the three groups.

Renal PPARδ and Bcl-6 expression. We found PPARδ mRNA and protein expression in the kidneys. At 8 weeks,

TABLE 1
Metabolic data at 8 weeks after inducing diabetes

	Control	DM	DM+GW0742
n	6	7	7
Systolic blood pressure (mmHg)	97.8 ± 7.9	111.8 ± 4.4	110.1 ± 3.5
HbA_{1c} (%)	4.60 ± 0.04	9.75 ± 0.34*	8.81 ± 0.62*
Body weight (g)	26.75 ± 0.39	17.74 ± 1.03*	20.70 ± 0.41*†
Kidney weight (mg)	283.3 ± 3.3	325.7 ± 18.8‡	295.7 ± 6.1
Relative kidney weight (mg/g body wt)	11.82 ± 0.27	18.85 ± 1.87*	15.87 ± 0.57
Creatinine clearance (mL/min)	249.0 ± 34.8	349.5 ± 40.4	348.1 ± 44.7
Triglycerides (mg/dL)	23.6 ± 2.0	27.9 ± 7.3	21.5 ± 4.8

Data are means ± SE. *$P < 0.01$ vs. the control group. †$P < 0.01$ vs. the DM group. ‡$P < 0.05$ vs. the control group.

renal PPARδ mRNA expression was significantly greater in the DM group than in the control group (0.71 ± 0.18 vs. 0.24 ± 0.07, respectively; $P < 0.05$) (Fig. 1*B*). However, GW0742 treatment did not affect PPARδ mRNA expression in renal tissues. Renal sections immunostained with PPARδ-specific antibodies revealed that PPARδ protein expression was predominantly localized in the glomeruli of DM and DM+GW0742 groups and to a lesser extent in the glomeruli of the control group (Fig. 1*C*). By contrast, the anti-inflammatory corepressor Bcl-6 was mainly expressed in the glomeruli of the control group, and its expression was suppressed in the DM group. GW0742 treatment recovered the expression of Bcl-6 compared with the DM group (Fig. 1*D*).

MMI and expression of type IV collagens in the glomeruli. Representative glomeruli in PAM-stained sections are shown in Fig. 2*A*. Glomerular hypertrophy and mesangial matrix expansion were observed in the DM group at the end of the 8-week observation period. However, these changes were ameliorated in the DM+GW0742 group compared with DM group (MMI: 9.05 ± 0.30 vs. 12.34 ± 0.49%, respectively; $P < 0.001$) (Fig. 2*B*). A similar trend was noted for type IV collagen (Fig. 2*C*). The type IV collagen–positive area in glomeruli was larger in the DM group than in the control group. This area was markedly reduced in the DM+GW0742 group compared with the DM group (9.57 ± 0.18 vs. 12.33 ± 0.49%, respectively; $P < 0.001$) (Fig. 2*D*).

Macrophage infiltration in the kidney. The number of macrophages in the glomeruli was remarkably higher in the DM group than in the control group. Interestingly, macrophage infiltration into the glomeruli was significantly reduced in the DM+GW0742 group compared with the DM group (1.80 ± 0.08 vs. 2.69 ± 0.05, respectively; $P < 0.001$) (Fig. 3*A* and *B*). Similarly, macrophage infiltration into the interstitium was increased in the DM group but was suppressed in the DM+GW0742 group (13.79 ± 0.53 vs. 7.75 ± 0.77, respectively; $P < 0.001$) (Fig. 3*A* and *C*).

Macrophage and inflammatory gene expression in the renal cortex. qRT-PCR analyses of kidney tissue demonstrated that the expression of two macrophage marker genes, *CD14* and *CD11c*, was increased in the DM group and that GW0742 treatment markedly reduced the expression of these genes (Fig. 4). *CD14* is a marker for all macrophages, and *CD11c* is specific for the M1 subtype of macrophages. Similarly, the induction of diabetes increased the renal expression of several proinflammatory and proatherogenic genes, including *MCP-1*, *TGF-β*, *OPN*, *TNF-α*, and *ICAM-1*. Although GW0742 decreased the expression of *MCP-1*, *TGF-β*, and *OPN*, it did not affect *TNF-α* or *ICAM-1* (Fig. 4). Of note, *MCP-1*, a key chemokine involved in macrophage recruitment, plays a significant role in diabetic nephropathy because the absence of *MCP-1* significantly reduces diabetic renal injury (18,19). Similarly, *OPN* is also a critical inflammatory cytokine involved in diabetic nephropathy (20,21). Collectively, these data indicate that the PPARδ agonist GW0742 inhibits diabetes–induced macrophage recruitment and inflammatory gene expression in the kidney.

PPARδ and Bcl-6 expression in RAW macrophages. PPARδ has been demonstrated to directly affect the anti-inflammatory transcriptional repressor Bcl-6. PPARδ agonists increase free Bcl-6 in macrophages, suppressing MCP-1 transcription and decreasing macrophage infiltration (22). To investigate the regulation of renal inflammatory pathways by diabetes and PPARδ, and the roles of Bcl-6 and PPARδ in these processes, we performed in vitro

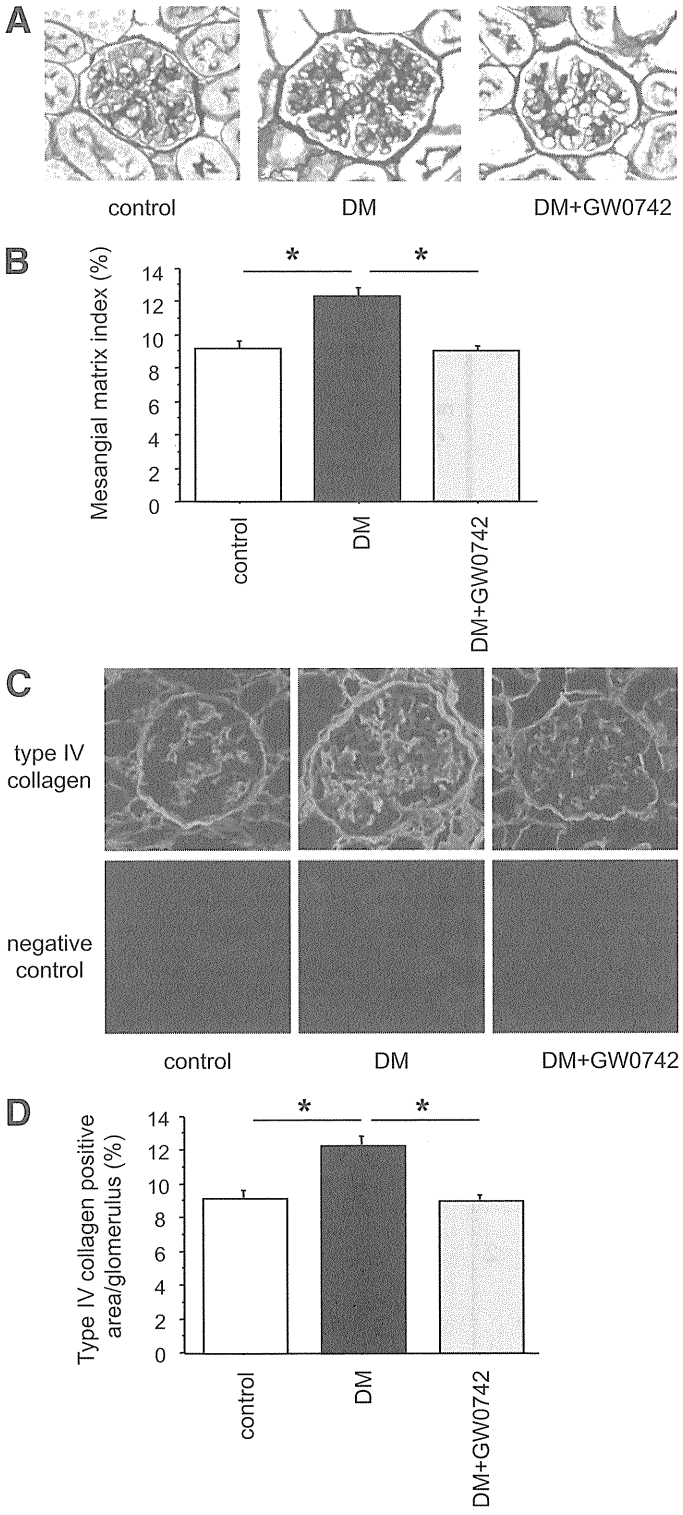

FIG. 2. PAM staining of kidney sections and the expression of type IV collagen in the kidney. *A*: Representative glomeruli from control, DM, and DM+GW0742 mice. Glomerular hypertrophy and mesangial matrix expansion were evident in the DM group. GW0742 suppressed the increase in the MMI compared with the DM group. Original magnification ×400. *B*: MMI in glomeruli. Data are means ± SE. *$P < 0.001$. *C*: Type IV collagen was significantly increased in the DM group compared with the control group and was decreased in the DM+GW0742 group compared with the DM group. Original magnification ×400. *D*: Type IV collagen–positive area in glomeruli. Data are means ± SE. *$P < 0.001$. (A high-quality digital representation of this figure is available in the online issue.)

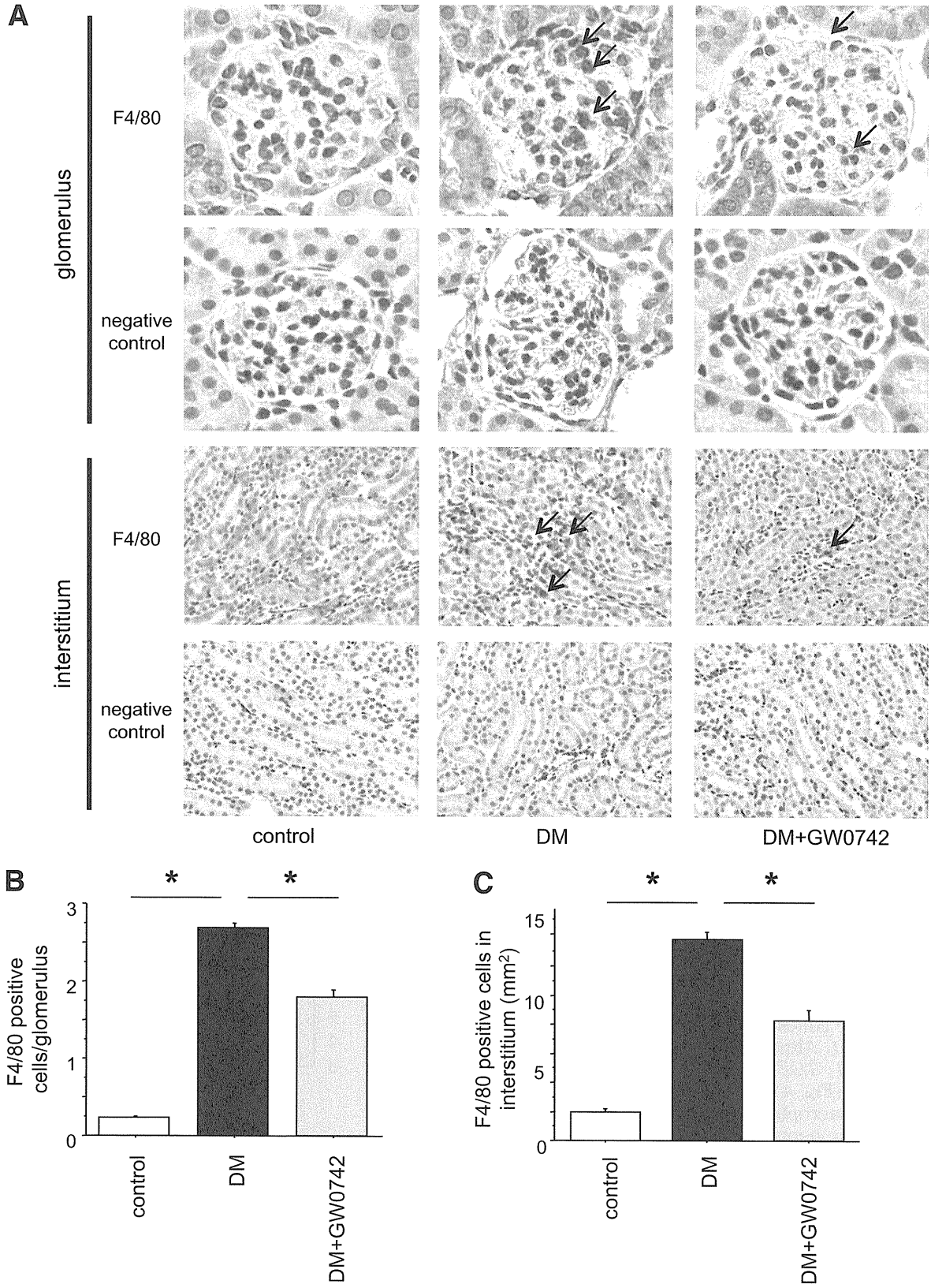

FIG. 3. Macrophage infiltration into the kidney. *A*: Macrophage (*arrows*) infiltration into glomeruli and interstitium was remarkable in the DM group and was suppressed in the DM+GW0742 group. Original magnification ×400. *B*: The number of intraglomerular macrophages. Data are means ± SE. *$P < 0.001$. *C*: The number of macrophages in interstitium. Data are means ± SE. *$P < 0.001$. (A high-quality digital representation of this figure is available in the online issue.)

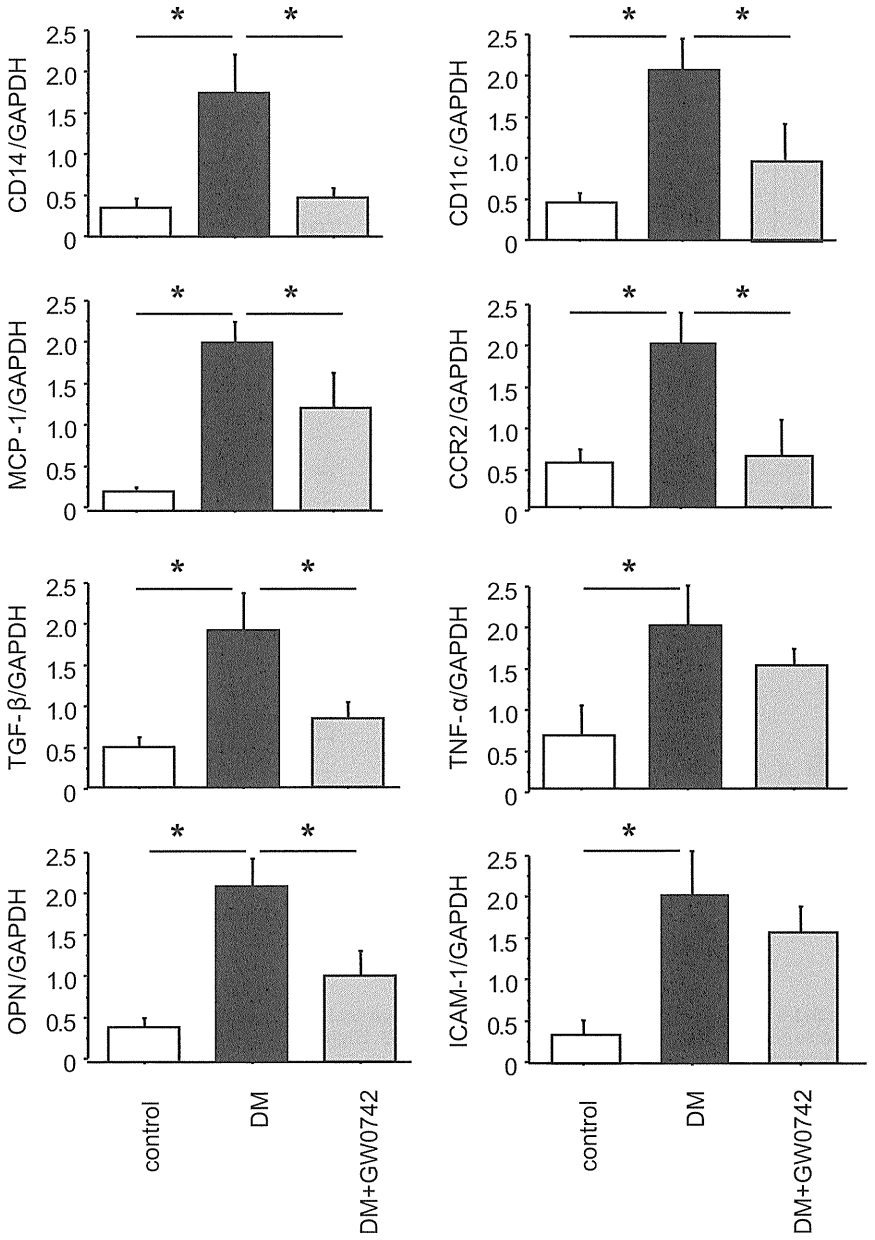

FIG. 4. PPARδ activation suppresses diabetes–induced renal inflammation and macrophage infiltration. Quantitative RT-PCR analysis of the expression of two macrophage markers (CD14 and CD11c) shows that GW0742 inhibited diabetes–induced macrophage infiltration into the kidney. Similarly, GW0742 suppressed MCP-1, CCR-2, TGF-β, and OPN mRNA levels in the kidney. mRNA levels are normalized to GAPDH. Data are means ± SE. *$P < 0.05$.

studies using RAW macrophages. qRT-PCR analyses revealed that the high-glucose medium strongly inhibited Bcl-6 expression in RAW macrophages and that GW0742 treatment significantly attenuated this inhibition in macrophages (Fig. 5*A*). We found that macrophages exposed to high glucose had an increase in nuclear PPARδ protein and that pretreatment with GW0742 completely abolished this effect (Fig. 5*B*). Western blot analyses of total and PPARδ-bound Bcl-6 in macrophage nuclear extracts revealed that high glucose tended to suppress total Bcl-6 but markedly increased PPARδ–Bcl-6 complexes and that GW0742 pretreatment decreased PPARδ–Bcl-6 binding (Fig. 5*C*). These data indicate that high glucose can increase nuclear PPARδ–Bcl-6 binding, limiting the amount of free Bcl-6 available to repress the expression of inflammatory genes normally suppressed by Bcl-6.

Inflammatory gene expression in RAW macrophages. To further investigate the role of PPARδ activation in inflammatory processes, we examined the effects of GW0742 on inflammatory gene expression in macrophages. Consistent with the changes in free Bcl-6, high glucose–stimulated MCP-1 expression, which is regulated by Bcl-6, was attenuated by GW0742 (Fig. 6*A*). The expression of OPN, a macrophage chemokine, was also increased by exposure to high glucose and suppressed by GW0742 (Fig. 6*B*).

DISCUSSION

In the current study, we demonstrated that the PPARδ agonist GW0742 ameliorated albuminuria, glomerular mesangial expansion, and type IV collagen accumulation without affecting blood glucose levels in STZ–induced

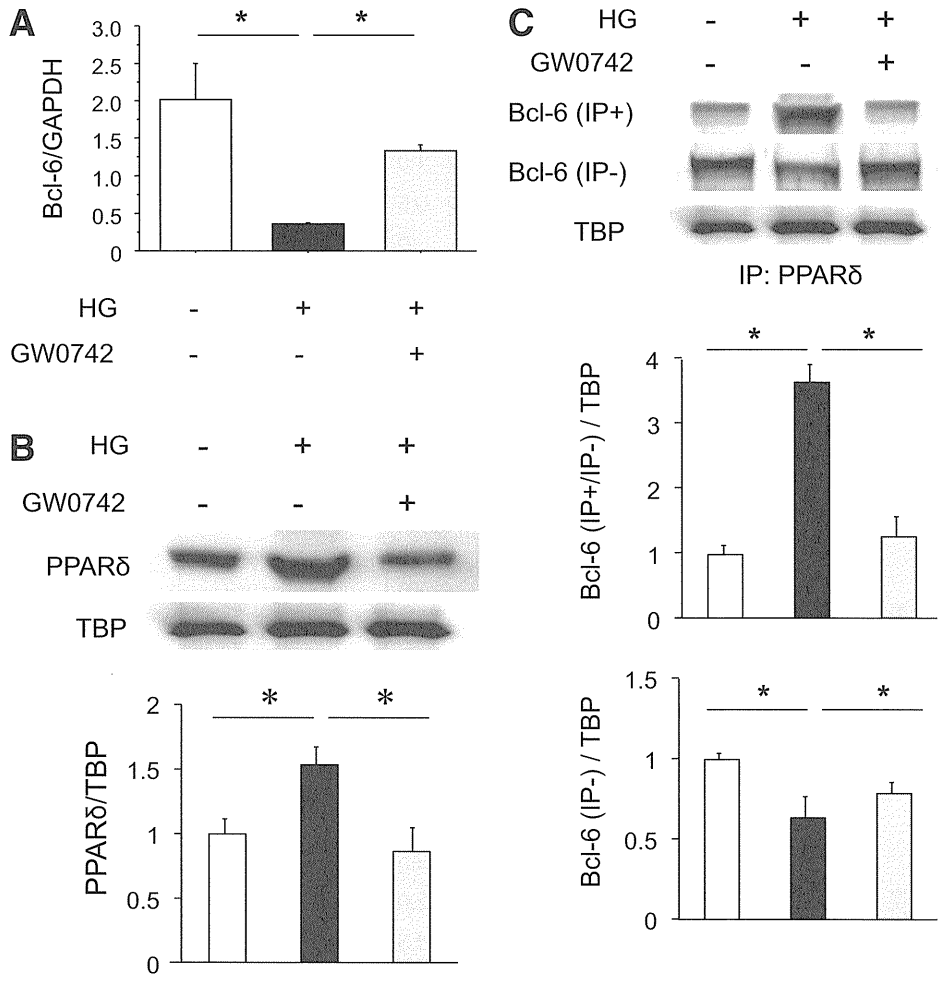

FIG. 5. High glucose suppresses Bcl-6 expression in RAW macrophages. *A*: mRNA isolated from macrophages was analyzed by quantitative RT-PCR. Bcl-6 expression was normalized to GAPDH. Data are means ± SE. **P* < 0.05. *B*: High glucose increases and GW0742 decreases macrophage PPARδ protein expression. PPARδ expression was normalized to that of TBP. Data are means ± SE. **P* < 0.05. *C*: Bcl-6 protein expression and PPARδ–Bcl-6 interaction in macrophages in response to high glucose and/or GW0742. The Bcl-6–PPARδ interaction was analyzed by Western blotting of total and PPARδ-bound Bcl-6 in macrophage nuclear proteins after pull-down assays. Bcl-6 expression was normalized to that of TBP. Data are means ± SE. **P* < 0.05.

diabetic mice. GW0742 treatment markedly decreased macrophage infiltration in diabetic kidney and the expression of inflammatory genes, including *MCP-1*, *TGF-β*, and *OPN*. Furthermore, in vitro studies with RAW macrophages revealed that high glucose suppressed the expression of free Bcl-6, which was associated with increased expression of MCP-1 and OPN, and that GW0742 reversed these effects. Our findings suggest that the activation of PPARδ

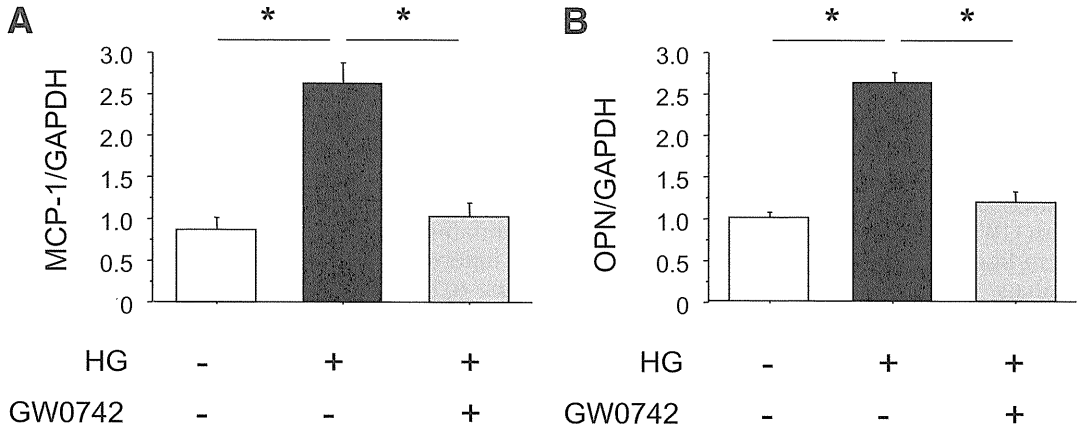

FIG. 6. GW0742 suppresses MCP-1 (*A*) and OPN (*B*) mRNA expression in RAW macrophages. mRNA isolated from macrophages was analyzed by quantitative RT-PCR. MCP-1 and OPN expression was normalized to GAPDH. Data are means ± SE. **P* < 0.05.

has an anti-inflammatory effect in diabetic kidneys and prevents the development of nephropathy, independently of blood glucose levels.

The nuclear receptor transcription factors PPARγ, PPARα, and PPARδ are critical in regulating insulin sensitivity, adipogenesis, lipid metabolism, and inflammation (11). All three PPAR isoforms have been proposed as therapeutic targets for the treatment of metabolic syndrome, dyslipidemia, and diabetes (11). Several recent clinical studies have provided evidence that thiazolidinedione, PPARγ agonists, and fibrates, PPARα agonists, confer a renoprotective effect in patients with type 2 diabetes (23–25). Experimental studies have also shown beneficial effects of PPARγ agonists on renal injury in type 1 and type 2 diabetic animal models, and multiple mechanisms seem to be involved (26,27). We previously demonstrated that the PPARγ agonist pioglitazone ameliorates diabetic nephropathy by inhibiting cell cycle–dependent hypertrophy of podocytes by reducing Bcl-2 and p27Kip1 protein levels (13) and by suppressing ICAM-1 expression and macrophage infiltration by inhibiting nuclear factor-κB activation in endothelial cells (14). PPARα agonists also have renoprotective effects by reducing TGF-β and plasminogen activator inhibitor-1 expression in mesangial cells (15). However, unlike PPARγ and PPARα, little is known about the therapeutic potential of PPARδ agonists in diabetic nephropathy.

Many studies have proposed an important role of inflammatory processes in the pathogenesis of diabetic nephropathy (6,7). We previously reported macrophage infiltration and increased expression of leukocyte adhesion molecules in the kidneys of patients with diabetic nephropathy in addition to mesangial matrix expansion and interstitial fibrosis (8). We have also described the importance of ICAM-1–dependent infiltration of macrophages into the kidney in the pathogenesis of diabetic nephropathy in a series of studies (9,28). Furthermore, we have demonstrated that SR-A–deficient mice are protected from renal injury after induction of diabetes by inhibiting macrophage migration into diabetic kidneys (10). Other studies have reported that the chemokine MCP-1 plays an important role in the pathogenesis of diabetic nephropathy (29). The importance of MCP-1 in the early development of diabetic nephropathy has been determined using animal models incorporating genetically deficient mice or therapeutic blockade of the MCP-1 receptor CCR2 (18,19,30). In the current study, MCP-1 expression in the kidney was increased in diabetic mice and suppressed by the administration of GW0742. PPARδ activation has been suggested to reduce MCP-1 and subsequently reduces the number of recruited macrophages in diabetic glomeruli and interstitium.

In this study, we found that diabetes significantly increased PPARδ expression in the kidney, and that high glucose increased PPARδ expression in cultured RAW macrophages. In contrast to our observations, Yu et al. (31) reported a decrease in PPARδ gene and protein expression in the myocardium of diabetic rats. On the other hand, several investigators observed an increase in PPARδ expression in the lung (32), diaphragm (33), and aorta (16) in diabetic animals. Taken together, these results suggest that PPARδ expression in the diabetic state differs between individual tissues and may depend on the balance between the two major fuel utilization pathways (i.e., glucose vs. fatty acid metabolism and their cross-talk) (33). The mechanisms by which high glucose increases the expression of PPARδ remain unclear, and further studies are needed.

Unliganded PPARδ, which binds to the anti-inflammatory transcriptional repressor Bcl-6, reduces the amount of free Bcl-6 available to suppress MCP-1 transcription, thus increasing MCP-1 expression (22). We showed that administration of the PPARδ agonist GW0742 substantially attenuated STZ–induced diabetic nephropathy without altering the blood glucose level and increased the renal expression of Bcl-6, which was associated with suppression of *MCP-1* gene expression in the kidney. We have searched for the PPRE in the promoter region of Bcl-6, but have been unable to locate any PPRE sites. Thus, we speculate that activation of PPARδ may induce other transcriptional factors, which induce *Bcl-6* gene expression. Moreover, immunoprecipitation and Western blotting revealed that high glucose increased the PPARδ–Bcl-6 complex, reducing the amount of free Bcl-6 in cultured macrophages. Activation of PPARδ by GW0742 decreased PPARδ–Bcl-6 binding and increased the amount of free Bcl-6, which consecutively decreased MCP-1 expression in macrophages. Based on these in vivo and in vitro data, inhibition of MCP-1 expression by PPARδ agonists is likely mediated through increased expression of Bcl-6 (Fig. 7).

OPN acts as a chemokine and as a proinflammatory cytokine (34). We previously demonstrated that OPN expression was increased in diabetic kidneys and suppressed by SR-A deficiency (10). Other studies have shown that OPN is expressed in renal resident cells and is regarded as

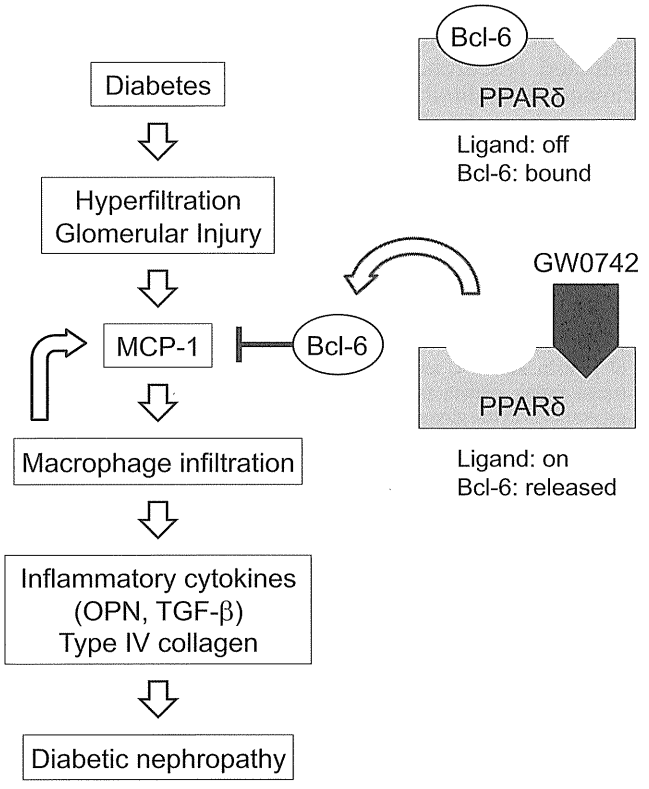

FIG. 7. Schematic diagram showing the mechanisms involved in the renoprotective effects of PPARδ in diabetic nephropathy. The anti-inflammatory transcriptional repressor Bcl-6 represses the expression of MCP-1. PPARδ activation by GW0742 releases Bcl-6, which is associated with suppression of MCP-1, to attenuate macrophage infiltration, inflammatory gene expression, and type IV collagen accumulation in the kidney.

a key molecule in the pathogenesis of diabetic nephropathy (20,21). In this study, consistent with the changes in MCP-1 expression, high glucose–induced OPN expression in macrophages was attenuated by GW0742. Therefore, inhibition of OPN expression by PPARδ agonists may contribute, at least in part, to the beneficial renal effects of PPARδ agonists in diabetic nephropathy.

In conclusion, the data presented in this study indicate that PPARδ activation attenuates high glucose–induced expression of MCP-1 and OPN by increasing the anti-inflammatory repressor Bcl-6 in macrophages. The PPARδ agonist GW0742 shows renoprotective effects through its anti-inflammatory activity by inhibiting MCP-1 expression and macrophage infiltration in the diabetic kidney. Because MCP-1 is a key component in the inflammatory response and the recruitment of monocytes/macrophages into the diabetic kidney, inhibition of MCP-1 expression by PPARδ agonist could provide a potential therapeutic target in human diabetic nephropathy.

ACKNOWLEDGMENTS

This study was supported in part by a Grant-in-Aid for Young Scientists (B) from the Ministry of Education, Culture, Sports, Science, and Technology, Japan, to D.O. (21790813). This work was supported by the Takeda Science Foundation and the Naito Foundation. No other potential conflicts of interest relevant to this article were reported.

Y.M. conducted the research and contributed to discussion. D.O. wrote the manuscript, conducted research, and contributed to discussion. J.W. contributed to discussion and reviewed and edited the manuscript. N.Y. conducted research. K.S. contributed to discussion. C.S., H.T., and N.T. conducted research. H.M. contributed to discussion and reviewed and edited the manuscript.

The authors thank Dr. Yasunori Takata (Ehime University, Japan) for helpful discussions.

REFERENCES

1. Declèves AE, Sharma K. New pharmacological treatments for improving renal outcomes in diabetes. Nat Rev Nephrol 2010;6:371–380
2. Dunlop M. Aldose reductase and the role of the polyol pathway in diabetic nephropathy. Kidney Int Suppl 2000;77:S3–S12
3. Koya D, Jirousek MR, Lin YW, Ishii H, Kuboki K, King GL. Characterization of protein kinase C beta isoform activation on the gene expression of transforming growth factor-beta, extracellular matrix components, and prostanoids in the glomeruli of diabetic rats. J Clin Invest 1997;100:115–126
4. Yang CW, Vlassara H, Peten EP, He CJ, Striker GE, Striker LJ. Advanced glycation end products up-regulate gene expression found in diabetic glomerular disease. Proc Natl Acad Sci U S A 1994;91:9436–9440
5. Sharma K, Ziyadeh FN. Hyperglycemia and diabetic kidney disease: the case for transforming growth factor-beta as a key mediator. Diabetes 1995; 44:1139–1146
6. Saraheimo M, Teppo AM, Forsblom C, Fagerudd J, Groop PH. Diabetic nephropathy is associated with low-grade inflammation in type 1 diabetic patients. Diabetologia 2003;46:1402–1407
7. Nelson CL, Karschimkus CS, Dragicevic G, et al. Systemic and vascular inflammation is elevated in early IgA and type 1 diabetic nephropathies and relates to vascular disease risk factors and renal function. Nephrol Dial Transplant 2005;20:2420–2426
8. Hirata K, Shikata K, Matsuda M, et al. Increased expression of selectins in kidneys of patients with diabetic nephropathy. Diabetologia 1998;41:185–192
9. Okada S, Shikata K, Matsuda M, et al. Intercellular adhesion molecule-1-deficient mice are resistant against renal injury after induction of diabetes. Diabetes 2003;52:2586–2593
10. Usui HK, Shikata K, Sasaki M, et al. Macrophage scavenger receptor-a-deficient mice are resistant against diabetic nephropathy through amelioration of microinflammation. Diabetes 2007;56:363–372
11. Lee CH, Olson P, Evans RM. Minireview: lipid metabolism, metabolic diseases, and peroxisome proliferator-activated receptors. Endocrinology 2003;144:2201–2207
12. Guan Y. Peroxisome proliferator-activated receptor family and its relationship to renal complications of the metabolic syndrome. J Am Soc Nephrol 2004;15:2801–2815
13. Okada T, Wada J, Hida K, et al. Thiazolidinediones ameliorate diabetic nephropathy via cell cycle-dependent mechanisms. Diabetes 2006;55:1666–1677
14. Ohga S, Shikata K, Yozai K, et al. Thiazolidinedione ameliorates renal injury in experimental diabetic rats through anti-inflammatory effects mediated by inhibition of NF-kappaB activation. Am J Physiol Renal Physiol 2007;292:F1141–F1150
15. Park CW, Zhang Y, Zhang X, et al. PPARalpha agonist fenofibrate improves diabetic nephropathy in db/db mice. Kidney Int 2006;69:1511–1517
16. Takata Y, Liu J, Yin F, et al. PPARdelta-mediated antiinflammatory mechanisms inhibit angiotensin II-accelerated atherosclerosis. Proc Natl Acad Sci U S A 2008;105:4277–4282
17. Barish GD, Atkins AR, Downes M, et al. PPARdelta regulates multiple proinflammatory pathways to suppress atherosclerosis. Proc Natl Acad Sci U S A 2008;105:4271–4276
18. Chow FY, Nikolic-Paterson DJ, Ozols E, Atkins RC, Rollin BJ, Tesch GH. Monocyte chemoattractant protein-1 promotes the development of diabetic renal injury in streptozotocin-treated mice. Kidney Int 2006;69:73–80
19. Chow FY, Nikolic-Paterson DJ, Ma FY, Ozols E, Rollins BJ, Tesch GH. Monocyte chemoattractant protein-1-induced tissue inflammation is critical for the development of renal injury but not type 2 diabetes in obese db/db mice. Diabetologia 2007;50:471–480
20. Susztak K, Böttinger E, Novetsky A, et al. Molecular profiling of diabetic mouse kidney reveals novel genes linked to glomerular disease. Diabetes 2004;53:784–794
21. Lorenzen J, Shah R, Biser A, et al. The role of osteopontin in the development of albuminuria. J Am Soc Nephrol 2008;19:884–890
22. Lee CH, Chawla A, Urbiztondo N, et al. Transcriptional repression of atherogenic inflammation: modulation by PPARdelta. Science 2003;302: 453–457
23. Iglesias P, Díez JJ. Peroxisome proliferator-activated receptor gamma agonists in renal disease. Eur J Endocrinol 2006;154:613–621
24. Sarafidis PA, Bakris GL. Protection of the kidney by thiazolidinediones: an assessment from bench to bedside. Kidney Int 2006;70:1223–1233
25. Fried LF, Orchard TJ, Kasiske BL. Effect of lipid reduction on the progression of renal disease: a meta-analysis. Kidney Int 2001;59:260–269
26. Isshiki K, Haneda M, Koya D, Maeda S, Sugimoto T, Kikkawa R. Thiazolidinedione compounds ameliorate glomerular dysfunction independent of their insulin-sensitizing action in diabetic rats. Diabetes 2000;49:1022–1032
27. Nicholas SB, Kawano Y, Wakino S, Collins AR, Hsueh WA. Expression and function of peroxisome proliferator-activated receptor-gamma in mesangial cells. Hypertension 2001;37:722–727
28. Sugimoto H, Shikata K, Hirata K, et al. Increased expression of intercellular adhesion molecule-1 (ICAM-1) in diabetic rat glomeruli: glomerular hyperfiltration is a potential mechanism of ICAM-1 upregulation. Diabetes 1997;46:2075–2081
29. Tesch GH. MCP-1/CCL2: a new diagnostic marker and therapeutic target for progressive renal injury in diabetic nephropathy. Am J Physiol Renal Physiol 2008;294:F697–F701
30. Kanamori H, Matsubara T, Mima A, et al. Inhibition of MCP-1/CCR2 pathway ameliorates the development of diabetic nephropathy. Biochem Biophys Res Commun 2007;360:772–777
31. Yu BC, Chang CK, Ou HY, Cheng KC, Cheng JT. Decrease of peroxisome proliferator-activated receptor delta expression in cardiomyopathy of streptozotocin-induced diabetic rats. Cardiovasc Res 2008;80:78–87
32. Huang CJ, Liu IM, Cheng JT. Increase of peroxisome proliferator-activated receptor delta gene expression in the lungs of streptozotocin-induced diabetic rats. Pulm Pharmacol Ther 2007;20:69–74
33. Salvi N, Guellich A, Michelet P, et al. Upregulation of PPARbeta/delta is associated with structural and functional changes in the type I diabetes rat diaphragm. PLoS ONE 2010;5:e11494
34. Denhardt DT, Giachelli CM, Rittling SR. Role of osteopontin in cellular signaling and toxicant injury. Annu Rev Pharmacol Toxicol 2001;41: 723–749

Clin Exp Nephrol (2011) 15:212–219
DOI 10.1007/s10157-010-0388-7

ORIGINAL ARTICLE

Intercellular adhesion molecule-1 plays a critical role in glomerulosclerosis after subtotal nephrectomy

Yuichi Kido · Daisuke Ogawa · Kenichi Shikata · Motofumi Sasaki · Ryo Nagase · Shinichi Okada · Hitomi Usui Kataoka · Jun Wada · Hirofumi Makino

Received: 4 February 2010 / Accepted: 21 November 2010 / Published online: 23 December 2010

Abstract
Background Hyperfiltration in the glomeruli have been considered to be an important cause of glomerular injury; however, the role of intercellular adhesion molecule (ICAM)-1 in the pathogenesis of glomerulosclerosis is not known.
Methods To elucidate the effects of ICAM-1 depletion on hyperfiltration-induced glomerular disorder, we used subtotally nephrectomized ICAM-$1^{+/+}$ and ICAM-$1^{-/-}$ mice. We evaluated macrophage infiltration, mesangial matrix expansion, transforming growth factor (TGF)-β and type IV collagen accumulation in glomeruli.
Results Macrophage infiltration into the glomeruli and mesangial matrix expansion coincident with increased expression of both ICAM-1 and TGF-β, and accumulation of type IV collagen were ameliorated in subtotally nephrectomized ICAM-$1^{-/-}$ mice compared to ICAM-$1^{+/+}$ mice. ICAM-1 depletion significantly reduced hyperfiltration-induced glomerular injury after renal ablation.
Conclusions Our present findings suggest that glomerular hyperfiltration is the leading cause of glomerulosclerosis, and it is mediated, at least in part, by ICAM-1 expression and macrophage infiltration.

Keywords ICAM-1 · TGF-β · Type IV collagen · Macrophage · Inflammation

Y. Kido and D. Ogawa equally contributed to this work.

Y. Kido · D. Ogawa · K. Shikata (✉) · M. Sasaki · R. Nagase · S. Okada · H. Usui Kataoka · J. Wada · H. Makino
Department of Medicine and Clinical Science, Okayama University Graduate School of Medicine, Dentistry and Pharmaceutical Sciences, 2-5-1 Shikata-cho, Kita-ku, Okayama 700-8558, Japan
e-mail: shikata@md.okayama-u.ac.jp

D. Ogawa
Department of Diabetic Nephropathy, Okayama University Graduate School of Medicine, Dentistry and Pharmaceutical Sciences, Okayama, Japan

H. Usui Kataoka
Department of Primary Care and Medical Education, Okayama University Graduate School of Medicine, Dentistry and Pharmaceutical Sciences, Okayama, Japan

K. Shikata
Center for Innovative Clinical Medicine, Okayama University Hospital, Okayama, Japan

Introduction

Intercellular adhesion molecule (ICAM)-1, a cell-surface protein with five immunoglobulin-like domains, is one of the major molecules, promoting leukocytes to attach firmly to endothelium followed by transmigration out of the blood vessel lumen [1]. ICAM-1 expression is upregulated in a variety of renal diseases, and infiltration of macrophages into the glomeruli is one of the characteristic features [2, 3]. Previously, we induced diabetes with streptozotocin (STZ) in ICAM-1-deficient (ICAM-$1^{-/-}$) and ICAM-$1^{+/+}$ mice and then monitored histopathological changes in the kidney over a period of 6 months [4]. The number of infiltrated macrophages was markedly reduced in diabetic ICAM-$1^{-/-}$ mice. Urinary albumin excretion, glomerular hypertrophy, and mesangial matrix expansion were more significantly ameliorated in diabetic ICAM-$1^{-/-}$ mice than in diabetic ICAM-$1^{+/+}$ mice. Moreover, expressions of transforming growth factor (TGF)-β and type IV collagen in glomeruli were also reduced in diabetic ICAM-$1^{-/-}$ mice. These results strongly suggest the important role of ICAM-1 in the pathogenesis of diabetic nephropathy,

whereas the critical mechanisms underlying the induction of ICAM-1 expression and hyperfiltration followed by glomerular infiltration of macrophages is still poorly understood. In the present study, we examined the effects of ICAM-1 depletion on hyperfiltration-induced glomerular injury using the five-sixths nephrectomized mice.

Materials and methods

Animal model

Male ICAM-$1^{-/-}$ mice [5] and wild-type mice (C57BL/6J mice, ICAM-$1^{+/+}$ mice), aged 8 weeks, were purchased from Jackson Laboratory (Bar Harbor, ME, USA). They were subjected either to sham operation (sham) or subtotal nephrectomy (Nx). The Nx operation was performed by surgical resection of the upper and lower third of the right kidney and following the left nephrectomy. Mice were divided into four groups; (1) ICAM-$1^{+/+}$ Nx ($n = 6$), (2) ICAM-$1^{-/-}$ Nx ($n = 6$), (3) ICAM-$1^{+/+}$ sham ($n = 6$) and (4) ICAM-$1^{-/-}$ sham ($n = 6$). All mice had free access to standard chow and tap water. All procedures were performed according to the Guidelines for Animal Experiments at Okayama University Medical School, Japanese Government Animal Protection and Management Law (No. 105) and Japanese Government Notification on Feeding and Safekeeping of Animals (No. 6). Six months after the operation, all the mice were killed and kidneys obtained. Kidneys were weighed and fixed in 10% formalin for periodic acid–methenamine–silver (PAM) staining and the remaining tissues were embedded in OCT compound and immediately frozen in acetone cooled on dry ice for immunohistochemistry.

Metabolic data

Serum and urinary creatinine, urinary albumin concentration, systolic blood pressure and body weight were measured before killing. Urine collection was performed for 24 h with each mouse individually housed in a metabolic cage and having free access to food and water. Urinary albumin concentration was measured by nephelometry (Organon Teknika-Cappel, Durham, NC, USA). Creatinine clearance (Ccr) was calculated in individual mice. Blood pressure was measured by the tail-cuff method.

Antibodies

Rat anti-mouse monocyte/macrophage monoclonal antibody (F4/80) was purchased from Serotec Ltd. (Kidlington, Oxford, UK). Goat anti-mouse ICAM-1 polyclonal antibody (M-19) and rabbit anti-human TGF-β1, -β2, -β3 rabbit polyclonal antibody (H112) were purchased from Santa Cruz Biotechnology (Santa Cruz, CA, USA). Anti-mouse type IV collagen antibody was purchased from Chemicon International, Inc. (Temecula, CA, USA). Biotin-labeled goat anti-rat IgG antibody, FITC-labeled donkey anti-goat IgG antibody, biotin-labeled donkey anti-rabbit IgG antibody and FITC-labeled goat anti-rat IgG antibody were purchased from Jackson Immunoresearch Laboratories (West Grove, PA, USA).

Light microscopy

Kidney tissues obtained were fixed in 10% formalin and embedded in paraffin. Tissue sections were cut at 3-μm thickness, dewaxed and stained with PAM. Histological morphometry was performed as described previously [4]. Briefly, to evaluate glomerular size and mesangial matrix expansion, 10 randomly selected glomeruli in the cortex of each animal were examined under high magnification (×400). Glomerular size was obtained by measuring glomerular tuft. Glomerular tuft area was measured by manually tracing the glomerular tuft using PhotoShop version 6 (Adobe Systems, San Jose, CA, USA) and analyzed by National Institutes of Health (NIH) Image version 1.6. Mesangial matrix area was defined as the PAM-positive area within the tuft area. The mesangial matrix index represented the ratio of mesangial matrix area divided by the tuft area. The results are expressed as mean ± SE (μm^2).

Immunohistochemical staining

Immunofluorescence and immunoperoxidase stainings were performed as described previously [4, 6]. Briefly, 4-μm thick fresh frozen sections were used for immunohistochemical study. To evaluate macrophage infiltration, frozen renal sections were stained with rat monoclonal antibody against mouse monocyte/macrophage (F4/80) and intraglomerular F4/80 positive cells were counted in 10 glomeruli per animal. To assess the glomerular expression of ICAM-1, frozen sections were stained with goat anti-mouse ICAM-1 antibody. Micrographic fluorescence photos were obtained using confocal laser fluorescence microscope (LSM-510, Carl Zeiss, Jena, Germany). To investigate the expression of renal TGF-β, renal sections were incubated with rabbit polyclonal antibody to TGF-β. Ten glomeruli were examined per animal under high magnification (×400), and the TGF-β positive area in a glomerulus was measured using NIH Image software. The TGF-β positive area of each glomerulus was expressed relative to the mean value of TGF-β positive areas in ICAM-$1^{+/+}$ sham mice. To evaluate the amount of glomerular type IV collagen, rabbit anti-type IV collagen antibody was used to visualize glomerular type IV collagen in the frozen section. Quantification of type IV

collagen immunofluorescence intensity was performed as follows. Color images were obtained as PICT files from the LSM-510. Image files in PICT format were inverted and opened in gray-scale mode using NIH image. The type IV collagen expression was calculated using the formula [X (density) $\times$ positive area (μm^2)]. The type IV collagen expression of each glomerulus was expressed as the ratio to the mean expression in ICAM-$1^{+/+}$ sham mice. Ten glomeruli were examined per animal for type IV collagen expression (total 60 glomeruli for each group).

Statistical analysis

All data were expressed as mean ± SEM. One-way analysis of variance (ANOVA) followed by Scheffe method was used to compare the means of group data. A P value <0.05 denoted the presence of a statistically significant difference.

Results

Metabolic data at the end of 6-month observation period

Six months after operation, there was no significant difference in systolic blood pressure, body weight, Ccr and urinary albumin excretion among the four groups (Table 1).

Expression of ICAM-1 and infiltration of macrophages

ICAM-1 protein expression was prominently upregulated in the glomeruli of ICAM-$1^{+/+}$ Nx mice, whereas ICAM-1 staining was not detectable in the glomeruli of both sham and Nx groups of ICAM-$1^{-/-}$ mice (Fig. 1). Infiltration of macrophages into glomeruli was significantly suppressed in ICAM-$1^{-/-}$ Nx mice compared with ICAM-$1^{+/+}$ Nx mice ($P < 0.0001$) (Fig. 1).

Light microscopy

Representative findings of glomeruli in PAM stained sections are shown in Fig. 2a. Severe glomerular hypertrophy and mesangial matrix expansion were observed in ICAM-$1^{+/+}$ Nx mice, whereas these histological abnormalities were ameliorated in ICAM-$1^{-/-}$ Nx mice. Sham operation did not induce any remarkable histological changes in PAM stained sections of ICAM-$1^{-/-}$ and ICAM-$1^{+/+}$ mice. Both glomerular and mesangial matrix areas were enlarged and mesangial matrix index was also increased in ICAM-$1^{+/+}$ Nx mice. These values were significantly decreased in ICAM-$1^{-/-}$ Nx mice (tuft area 4648 ± 127 vs. 6522 ± 307 μm^2, $P < 0.0001$, mesangial matrix area 218 ± 12 vs. 687 ± 50 μm^2, $P < 0.0001$, mesangial matrix index 4.9 ± 0.3 vs. 11.0 ± 0.9%, $P < 0.0001$, Fig. 2b–d).

Expression of TGF-β and type IV collagen

Subtotal nephrectomy induced the marked enlargement of TGF-β-positive area in the glomeruli of ICAM-$1^{+/+}$ mice, whereas the magnification of TGF-β-positive area was significantly reduced in the glomeruli of ICAM-$1^{-/-}$ Nx mice (724 ± 45 vs. 105 ± 9% of ICAM-$1^{+/+}$ sham mice, $P < 0.0001$, Fig. 3a, b). The enhancement of type IV collagen staining in the glomeruli of ICAM-$1^{+/+}$ Nx mice was also significantly ameliorated in ICAM-$1^{-/-}$ Nx mice (297 ± 13 vs. 106 ± 5.5% of ICAM-$1^{+/+}$ sham mice, $P < 0.0001$, Fig. 3a, c).

Discussion

In the present study, ICAM-$1^{-/-}$ and ICAM-$1^{+/+}$ mice were subjected either to sham operation or to subtotal nephrectomy and physiological and histopathological findings for the progression of glomerular injury were then evaluated. Subtotal nephrectomy is a model of chronic glomerular disorder with hyperfiltration of a single glomerulus [7]. Six months after operation, there was no significant difference in systolic blood pressure, Ccr and urinary albumin excretion among the four groups (Table 1). These results suggest the increased single nephron blood flow and GFR in Nx groups because the Nx groups exhibited similar Ccr to the sham groups with reduced number of nephrons. Histopathological observation of ICAM-$1^{-/-}$

Table 1 Metabolic data in each experimental group

Genotype	Sham operated mice		Nephrectomized mice	
	ICAM-$1^{+/+}$	ICAM-$1^{-/-}$	ICAM-$1^{+/+}$	ICAM-$1^{-/-}$
n	6	6	6	6
Systolic blood pressure (mmHg)	107.5 ± 7.2	100.1 ± 7.8	102.6 ± 4.1	105.6 ± 5.9
Body weight (g)	30.4 ± 2.9	29.3 ± 2.1	29.4 ± 1.9	29.7 ± 0.9
Creatinine clearance (ml/min/g body wt)	5.5 ± 3.1	5.8 ± 3.2	4.7 ± 1.5	5.8 ± 1.7
Urinary albumin excretion (mg/day)	3.2 ± 0.3	3.3 ± 0.5	10.9 ± 1.7	8.3 ± 1.2

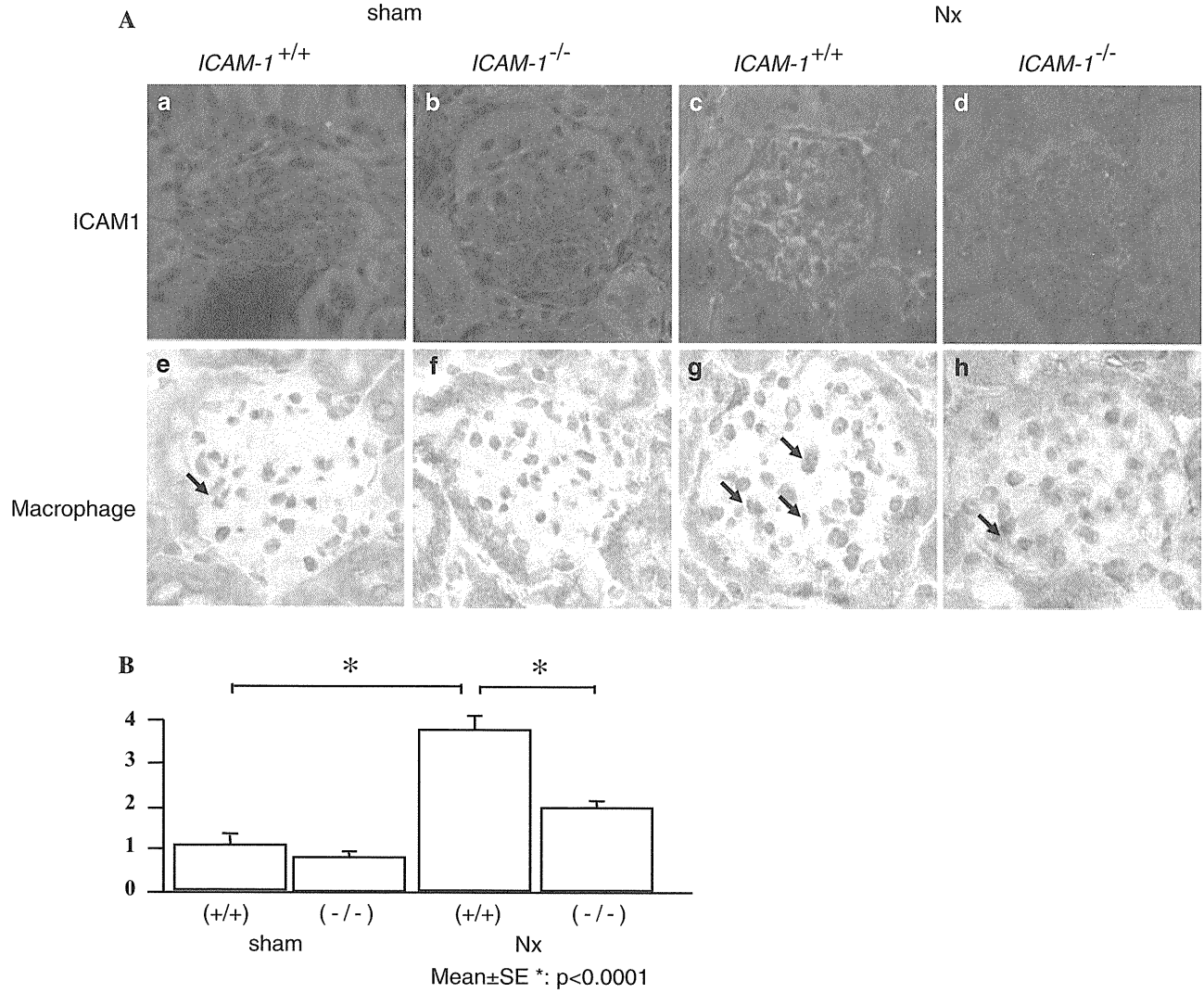

Fig. 1 Expression of ICAM-1 in the glomeruli, macrophage infiltration into the glomeruli and number of macrophages in the glomeruli. **A** ICAM-1 expression is increased in the glomeruli of ICAM-$1^{+/+}$ nephrectomized (Nx) mice (**c**) compared with the glomeruli of sham operation groups (**a**, **b**), whereas ICAM-1 is not stained in ICAM-$1^{-/-}$ Nx mice glomeruli (**d**). *Arrows* depict macrophages infiltrated into the glomeruli (**e**–**h**). The number of infiltrated macrophages is prominently increased in the glomeruli of ICAM-$1^{+/+}$ Nx mice (**g**) and inhibited by ICAM-1 depletion (**h**) whereas the staining for macrophages is rarely found in the glomeruli of sham operated mice (**e**, **f**). ×400. **B** The quantitative analysis for the number of intraglomerular macrophages. Data are mean ± SEM, $*P < 0.0001$, +/+, ICAM-$1^{+/+}$ mice; −/−, ICAM-$1^{-/-}$ mice

mice revealed the ameliorated glomerular infiltration of macrophages associated with up-regulation of ICAM-1 expression induced by subtotal nephrectomy (Fig. 1). Mesangial matrix expansion (Fig. 2), overproduction of TGF-β and accumulation of type IV collagen (Fig. 3) in the glomeruli of Nx mice were significantly reduced in ICAM-$1^{-/-}$ mice.

The phenotypes of ICAM-$1^{-/-}$ mice used in this study were originally reported by Sligh et al. [5]. ICAM-$1^{-/-}$ mice are fertile without any apparent developmental defects. They exhibit impaired immunoresponses, i.e., impaired neutrophil emigration in response to chemical peritonitis and decreased contact hypersensitivity, whereas any obvious abnormal phenotype has not been reported in normal conditions with exceptions of increased number of circulating neutrophils and body weight [8, 9]. In the kidney, ICAM-1 expression is up-regulated in human glomerulonephritis [10] and in a variety of experimental animal models of renal diseases, including crescentic glomerulonephritis [11, 12], renal ablation [13], and autoimmune glomerulonephritis [14, 15]. We reported that blocking antibodies against ICAM-1 prevent leukocyte influx into the glomeruli in experimental glomerulonephritis [12] and renal ablation model [13]. Furthermore, we demonstrated that the up-regulation of ICAM-1 is associated with infiltration of leukocytes, mainly macrophages, in

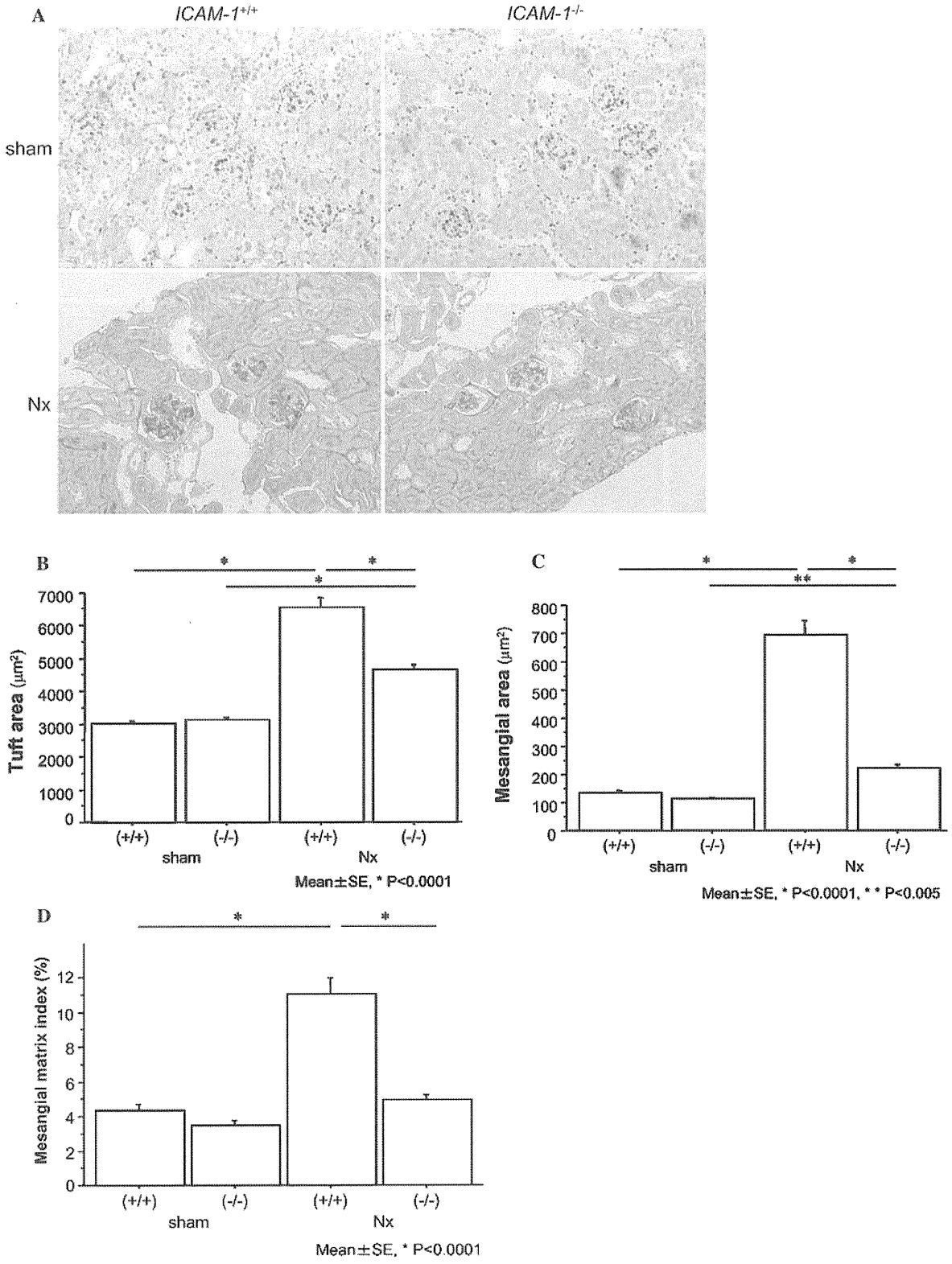

Fig. 2 PAM and azan staining of glomeruli. **A** PAM staining of mice glomeruli indicates the glomerular hypertrophy and mesangial matrix expansion, prominent in the glomeruli of ICAM-$1^{+/+}$ Nx mice (**c**) compared with the ICAM-$1^{-/-}$ Nx mice glomeruli (**d**). ×400. **B** The areas of glomerular tuft. **C** The areas of mesangial matrix. **D** Mesangial matrix index. Change in the amount of mesangial matrix was evaluated using the ratio of PAM-positive area in the tuft area as described in the "Materials and methods". ICAM-1 abrasion resulted in the decreased extent of mesangial matrix index up-regulation induced by subtotal nephrectomy. Data are mean ± SEM, $*P < 0.0001$, $**P < 0.005$, +/+, ICAM-$1^{+/+}$ mice; −/− ICAM-$1^{-/-}$ mice